TRANS BLACK SEA REGION UNION OF
APPLIED ELECTRODYNAMICS (BSUAE)

R. Zaridze, G. Bit-Babik, D. Karkashadze
R. Jobava, D. Economou and N. Uzunoglu

THE METHOD OF AUXILIARY SOURCES (MAS)

Solution of Propagation, Diffraction and Inverse Problems Using MAS

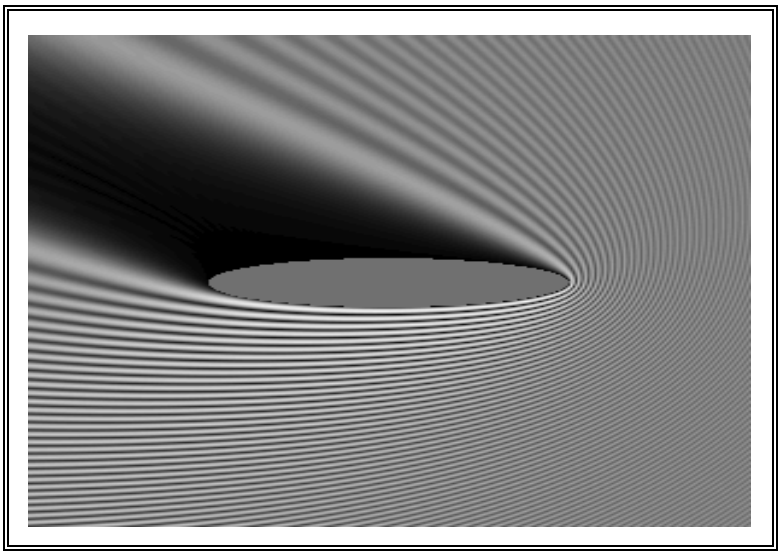

Tbilisi - Athens
1998

Printed by
Institute of Communication and
Computers Systems, Athens, Greece
Tel: +301 7723556, Fax: +3017723557

ISBN

Athens, Greece
February, 1998

Preface

The method of Auxiliary Sources (MAS) is presented in the following scientific book with the aim to introduce this method to researchers working in the field of Computational Electromagnetics. During the last twenty years three fundamental methods :

Method of Moments
Finite Element, and
Finite Differences Time Domain

have been proposed in western countries to analyze accurately arbitrary electromagnetic structures. The MAS has been developed following the principal concepts lead by famous Georgian School of Mathematical Physics and is little known outside of ex-USSR countries.

In the following chapters details of implementing MAS in various electromagnetic computational techniques is presented. It is hoped that the information in the following chapters will invoke the interest of researchers to apply this method in coping with practical problems as well as to combine this method with other computational electromagnetic methods to develop more accurate and advance techniques.

The main results given in this book were presented at the Trans Black Sea Region Symposium on Applied Electromagnetism in Metsovo, Epirus Greece on April 17-19, 1996 and in the NATO Advanced Study Institute in Applied Computational Electromagnetics held on July 26 - August 5, 1997 in Samos, Greece.

This book could be useful for graduate and postgraduate electrical engineering and physics students as well as for scientists working in the area of electromagnetics.

R. Zaridze and N. Uzunoglu

Abstract

The Method of Auxiliary Sources (MAS) for solution of Applied Electrodynamics problems is presented in this book. From mathematical viewpoint this method is based on the expansion of wave filed solution by non-orthogonal functions which are the fundamental solutions of the appropriate wave equation. The book reviews the General MAS algorithm which successfully have been used in last 30 years for solution of the mathematical physics boundary problems as well as the recent developments of the method and possible new applications.

The new results of investigations of physical properties of scattered fields are given. Using the fundamental properties of the solutions of wave equation some new approaches are suggested for solution of applied electrodynamics problems. Moreover, the consideration of these properties have been used for electromagnetic field reconstruction and visualization which expands the class of solved problems. The MAS is expanded for large body scattering problems minimizing at the same time the required computer resources. The new approach for solution of inverse problems base on the consideration of the traveling wave singularities is also discussed. Recommendations are made in order to use the MAS by electrical engineers for various applications.

Contents

Introduction

The development of high-speed multipurpose numerical techniques for solution of up-to-date applied electrodynamics and wave scattering problems is very important. The proposed solutions of such problems can be divided into three groups.

1. Analytical (exact or asymptotic) methods, which express the solution by elementary or special functions. Such solution can be found for very special and abstract cases, that are usually far from practice.

2. Numerical-analytical methods, which allow to reduce the problem of the integral equations to a system of linear equations. Then numerical algorithms can be implemented to obtain the solution of the initial problem.

3. Numerical methods which decrease the analytical processes by increasing the computational efforts.

From the engineering viewpoint the third method seems more attractive. Such methods are usually more flexible and universal than the analytical one. Because of different geometry and type of incident field the numerical methods seems to be the only tools that can satisfy the requirements of modern applications and computational experiments.

The essential features of the modern numerical methods can be enumerated as follows.

1) The universality of the method and algorithm. This means the possibility of solving problems with arbitrary complex geometry and any type of incident field.

2) The wide scope of the method. This means that the method should work with the wide range of input parameters of the system under investigation (for example the precision and calculation time must not be essentially increased while the incident field wavelength changes).

3) It is desirable that the method should be applicable to a variety of problems, including the case of resonance excitation, when the electrodynamics interaction between the system elements highly increases.

4) An important feature is the simplicity and ease of use of the method for engineering applications.

5) At last, in order to use numerical experiment, an important requirement is the speed of computational algorithm. The solution of a problem needs optimization of different parameters of the problem in order to achieve the best possible properties.

The Method of Auxiliary Sources was developed for solving a wide class of electrodynamics problems and as experience showed it satisfies most of the features and requirements mentioned above. This technique was used for simulation and computation of electrodynamics problems and was improved during the solution of numerous applied problems.

Mathematical justification of the method of auxiliary sources was done by the Georgian mathematicians (Kupradze [1-2], Vekua [3-5]). There is also a number of works which authors, probably independently, offered such representations of scattered fields [6-14].

Some of the authors considered such approach only as a mathematical way of constructing solutions of the physical problem and did not consider any physical meanings. The traditional practice was to use the MAS for boundary problem of mathematical physics without optimizing any auxiliary parameter. In [1,2] it is proved that for arbitrary closed

auxiliary surface inside area ***D*** the solution tends to the true one with the increasing of the number of auxiliary sources. Later during the solution of applied problems it has been shown that the basic difficulties arise unless all physical properties of the scattered field are taken into account in the algorithm and vice versa. Stability, and convergence depends on the correct choice of auxiliary parameters considering the physical meaning.

Conventional MAS was successfully used by many researchers for the solution of a wide group of applied problems - elasticity and geophysics, electrostatic problems, hydrodynamics, diffraction and propagation of acoustic and electromagnetic waves and so on. So the modern algorithm of the MAS is developed as a numerical method for the solution of boundary problems of mathematical physics [15-25].

Consideration of the physical properties of scattered field, gives the wide possibilities of the method. In this work the new results of investigations and expanded possibilities of the MAS will be presented. It is known that any wave field carrying the energy into infinity must have the centers of radiation, singularities in some area. Otherwise the wave fields value should be everywhere identically equal to zero [26]. In this paper attention is paid to localization of these singularities under assumption that every wave field is determined by its own singularities in a unique fashion. Investigations have shown that these singularities are distributed as a bright centers. The localization of singularities is used for partial representation of the scattered field sharply reducing the number of unknowns and for optimization of the Inverse Problems solution.

The investigations of diffraction problems on large 3-D bodies are receiving a considerable amount of attention. Creation of efficient method for numerical solution of these problems is of great practical interest. The modern computer resources still restrict the utilization of such well known methods as Method of Moments or finite-elements method and others because of memory and CPU-time limitations. Other works explore the hybridization of different methods [41]. This work presents the minimization of required computer resources for solution of 2-D problems. It is shown that for efficient utilization of this method the auxiliary sources must be placed in the region of the scattered field singularities. The information of this regions is contained in the problem conditions and can be obtained from scatterer geometry and the type of incident field.

Section I reviews the essence of the General MAS algorithm and gives an explanation of SFS. Section II describes the major problems that arise during the solution of applied electromagnetics problem using the MAS and solution of this problems based on the physical properties of wave functions. The new approach for solution of waveguide systems problem is presented. Section III presents the method based also on the MAS for SFS localization using the uniqueness of analytical continuation of the wave field. For this purpose in 2-D problems the functions $H_0^{(1)}(kr)$ and $H_0^{(2)}(kr)$ which describe the converging and diverging waves respectively are used. Based on these concepts and with the help of the MAS the simple numerical method for field reconstruction up to its singularities is suggested. It was shown that SFS are distributed as bright points nearby the caustic surface. This information of SFS localization is used for efficient solution of scattering problems on large bodies by partial representation of scattered field. Section IV describes the application of MAS and SFS consideration for inverse problems solution. Example is given for synthesize the radiator with desired pattern and minimum of reactive field in near zone, so that all feeding energy is transmitted into traveling wave. In the last section V the MAS in time domain is presented. This is an extension of the MAS which is conveniently used for transient diffraction problems. It provides a fast algorithm for simulation and visualization of electromagnetic periodical and transient processes in time domain.. As an example the transient scattering of EM pulse on the cylinder with longitudinal slot is considered.

I. The General Method of Auxiliary Sources

1. The Method of Auxiliary Sources

A fundamental diffraction problem is described as follows: A media with permittivity ε and permeability μ is excited by the incident wave U^i. The posed problem is to determine the vectors $\vec{E}$ and $\vec{H}$ of the EM field, which satisfy the Maxwell equations and the radiation condition. In the more complex case, these vectors must also satisfy the appropriate boundary conditions.

Suppose the perfectly conducting surface **S** of a scatterer that covers the area **D** (Fig. 1.1). Assuming a time dependence of $e^{-i\omega t}$ type the problem is reduced to finding out the solution of Helmholtz equation

$$\Delta U^s(x,y,z) + k^2 U^s(x,y,z) = 0\,, \quad (1.1)$$

which satisfies the boundary condition:

$$W\left\{U^s(x,y,z) - U^i(x,y,z)\right\} = 0,\ M(x,y,z) \in S\,, \quad (1.2)$$

where $U^i(x,y,z)$ is the incident field, $U^s(x,y,z)$ is the scattered field, W is the operator of the boundary conditions. Then, according [1], an auxiliary surface σ is introduced inside area **D** and on this surface is uniformly distributed a set of the points $\{x_n, y_n, z_n\}_{n=1}^{\infty} \in \sigma$.

Let $\left\{U(|\vec{r}_n - \vec{r}|)\right\}_{n=1}^{\infty}$ - be the Helmholtz equation's fundamental solutions by which the scattered field is to be represented. These functions are:

$$U(|\vec{r}_n - \vec{r}|) = H_0^{(1)}(k\sqrt{(x_n - x)^2 + (y_n - y)^2}) \quad \text{- 2-D} \quad (1.3)$$

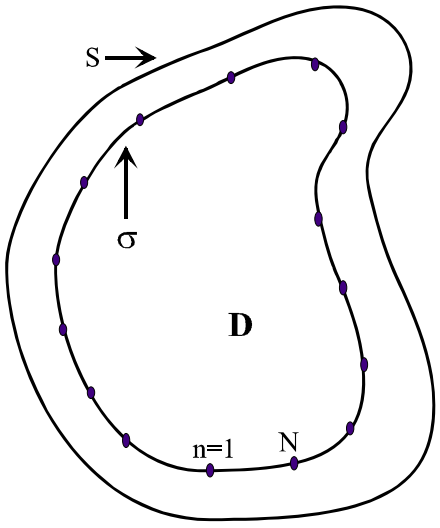

Figure 1.1: On the formulation of the problem

$$U(|\vec{r}_n - \vec{r}|) = \frac{e^{ikr_n}}{r_n} \quad \text{- 3-D} \quad (1.4)$$

where $|\vec{r}_n - \vec{r}_s| = \sqrt{(x_n - x_s)^2 + (y_n - y_s)^2 + (z_n - z_s)^2}$; $M(x_n, y_n, z_n) \in \sigma$;

It has been proved by V. Kupradze [1-2] that:

1. The system of functions **{** $\{U(|\vec{r}_n - \vec{r}|)\}_{n=1}^{\infty}$ **}** - Helmholtz equation's fundamental solutions - which describes the characteristics of the field (electric field, magnetic field, or field's potentials) ***are complete and linearly independent on the surface*** **S in L_2 space.**

2. There are such coefficients j_n that using the first N functions of the mentioned system, all kind of functions of scattered field on the surface **S** can be represented by a linear combination of the fundamental solutions with the appropriate coefficients:

$$U^i(x, y, z)\Big|_S \approx \sum_{n=1}^{N} j_n U(|\vec{r}_n - \vec{r}|)\Big|_S \quad (1.5)$$

Then, the approximate solution of the boundary problem is:

$$\tilde{U}^s(x, y, z) = \sum_{n=1}^{N} j_n U(|\vec{r}_n - \vec{r}|) \quad (1.6)$$

outside ***D*** and will tend to exact solution $U^s(x,y,z)$ as $N \to \infty$. This is the essence of the conventional MAS introduced by Kupradze.

Similar properties posses a systems of multiple sources functions which have been considered by I. Vekua [3,4,5] for solution of boundary problems with cylindrical symmetry:

$$\left\{H_n^{(1)}(k\rho)\, e^{in\varphi}\right\}_{n=1}^{\infty}$$

Here $H_n^{(1)}(k\rho)$ are the first kind Hankel functions of the order **n**. The two approaches could

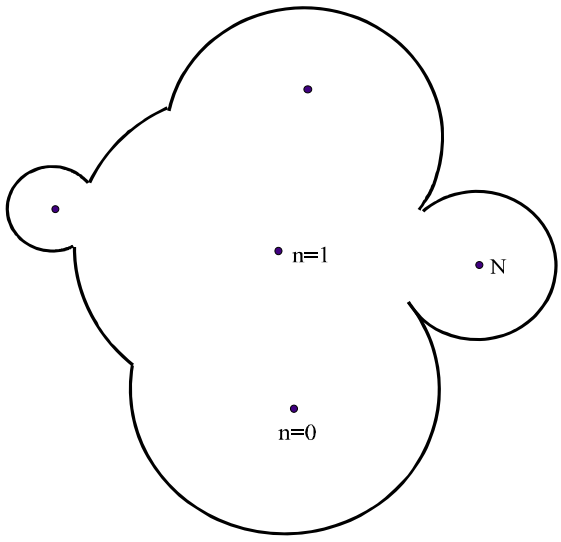

Figure 1.2: Complex cross-section

be proved to be identical using the additional theorem for cylindrical functions.

In case of closed surface, when the cross-section of the cylindrical body is circular or consists of the parts of circular cylinders [23] (fig. 1.2), Hankel functions of higher orders are more convenient. In general case we use:

$$U^{s}(r) = \sum_{n=0}^{N} \sum_{m=-M}^{M} a_{nm} H_{m}^{(1)}(k r_n) e^{im\varphi} \quad (1.7)$$

the origins of coordinates are in the centers of curvature inside the surface **S**.

In case of the bodies with complex cross sections, especially when the surface is open and has edges, Helmholtz equation's fundamental solutions are more universal.

In case of dielectric scatterer (see fig. 1.3) when the scattered field should be found along with the field inside the body, two auxiliary surface must be chosen on the both side of the major surface [27, 28]. One of them, located inside will determine the field outside (similar to conducted body) and sources, distributed outside determine the field inside the dielectric body. On each of these surfaces the *N* Auxiliary Sources are distributed, which vector-potentials are presented by the fundamental solution of the Helmholtz equation: $U(k\sqrt{\varepsilon\mu}|\vec{r}_n - \vec{r}|)$, where ε and μ are permittivity and permeability of corresponding media, $\vec{r}_n$ - the points where the Auxiliary Source is located and $\vec{r}$ - the observation point. The unknown electric and magnetic field are expressed by this Auxiliary Sources as sum with unknown coefficients:

$$E(\vec{r}) = \hat{w}_e \left\{ \sum_{n=1}^{N} a_n U\left(k\sqrt{\varepsilon\mu}|\vec{r}_n - \vec{r}|\right) \right\} \quad (1.8)$$

$$H(\vec{r}) = \hat{w}_h \left\{ \sum_{n=1}^{N} a_n U\left(k\sqrt{\varepsilon\mu}|\vec{r}_n - \vec{r}|\right) \right\} \quad (1.9)$$

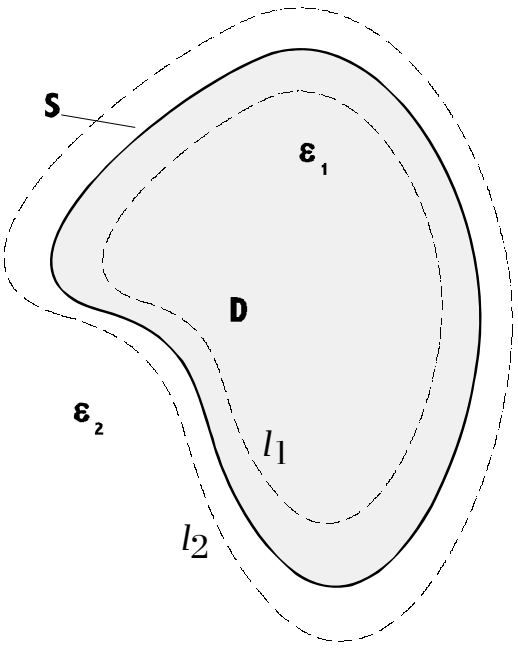

Figure 1.3: Dielectric scattered

where $\hat{w}_e$ and $\hat{w}_h$ are the operators for calculating the unknown electric and magnetic field respectively from vector-potentials. It should be stated again that the field inside the dielectric are found by the *N* Auxiliary Sources placed outside the scatterer and vice versa.

If the scatterer is illuminated by the incident field $U^{inc}(\vec{r})$, the boundary condition could be written as follows:

$$\begin{cases} \hat{W}_e\left[\sum_{n=1}^{N} a_n^{out} U\left(k\sqrt{\varepsilon_1\mu_1}\left|\vec{r}_n-\vec{r}\right|\right)-\sum_{n=1}^{N} a_n^{in} U\left(k\sqrt{\varepsilon_2\mu_2}\left|\vec{r}_n-\vec{r}\right|\right)\right]=E_\tau^{inc}(\vec{r})\big|_S \\ \hat{W}_h\left[\sum_{n=1}^{N} a_n^{out} U\left(k\sqrt{\varepsilon_1\mu_1}\left|\vec{r}_n-\vec{r}\right|\right)-\sum_{n=1}^{N} a_n^{in} U\left(k\sqrt{\varepsilon_2\mu_2}\left|\vec{r}_n-\vec{r}\right|\right)\right]=H_\tau^{inc}(\vec{r})\big|_S \end{cases}, \quad (1.10)$$

where $\hat{W}_e$ and $\hat{W}_h$ is the operators of boundary condition, a_n^{in} and a_n^{out} are the coefficients of the Auxiliary Sources placed inside and outside the dielectric scatterer respectively and $E_\tau^{inc}(\vec{r})$ and $E_\tau^{inc}(\vec{r})$ are the tangential components of the incident field on the boundary surface *S*. If $2N$ collocation points are chosen on the major surface *S* the (1.10) gives the system of $2N \times 2N$ linear equations. Solving this system the coefficients a_n^{in} and a_n^{out} will be obtained, so the unknown scattered field could be constructed according to (1.8) and (1.9). Again in the conventional MAS the approximate solution presented by equations (1.8) and (1.9) tends to exact solution with increasing of the number *N* of points.

2. On the Shifting of Auxiliary Surface

Taking into account the above discussion can note that for the representation of the scattered field outside the body the auxiliary surface is always shifted inside the scatterer. In case of dielectric the surface that describes the field outside the scatterer is shifted inside the boundary surface and the one describing the field inside the scatterer is shifted outside. It is important to emphasize the significance of such shifting.

Following the integral equations method, the solution of the boundary problems is reduced to the singular integral equation [26].

$$U^i\big|_S = \int_s a(s)U(kr_s)\,ds \quad (1.11)$$

where U^i is the value of the incident field on the surface *S* of the body. The function $a(s)$ is the value of the current distribution on the surface of the body.

Notice that the difference between equation (1.11) and (1.12) (the limit case of equation (1.5) when $N \to \infty$) is that the integrating function in (1.11) has singularities in the integrating surface while there no singularities in equation (1.12) due to the shifting of the auxiliary surface.

$$U^i(x,y,z)_S = \lim_{N\to\infty}\sum_{n=1}^{N} j_n U\left(\left|\vec{r}_n-\vec{r}\right|\right)\Big|_S = \int j(\sigma)U\left(k\left|\vec{r}_n-\vec{r}_\sigma\right|\right) \quad (1.12)$$

Both terms in equation (1.12) are same if the auxiliary surface coincides with the surface *S* of the scatterer.

The singularity in equation (1.11) forces one to use the various techniques to calculate the current distribution $a(s)$. If the auxiliary surface coincides with surface of scatterer then the singularity occurs in this case too. The shifting of the auxiliary surface automatically helps to avoid this, so the solution is obtained easily.

Another advantage of shifting is the convergence of the solution. Using MAS the integral is replaced with a summation. The accuracy depends on the number of terms in this summation. On the fig. 1.4 the convergence of solution for different shifts is shown. It is shown that the accuracy is improved for constant number of auxiliary sources while the depth of the auxiliary surface increases. This can be explained by the fact that shifting of Auxiliary Sources inside the scatterer makes the scattered field function more smooth on the surface of the body and its identity with the incident field in the collocation points remains in other points of the surface, i.e. the fulfillment of the boundary conditions in the region between collocation points is improved.

However this is valid only up to a certain depth [17, 22], after which the convergence sharply gets worse and might even diverge (fig. 1.5a, 1.5b). This occurs if the auxiliary surface does not enclose all Scattered Field Singularities. The physical meaning of this observation is that in this case the field in the region of singularity can not represented by auxiliary sources.

Next the expansion coefficients has to be determined. Various techniques have been implemented for this purpose. In the case of the collocation technique, the boundary

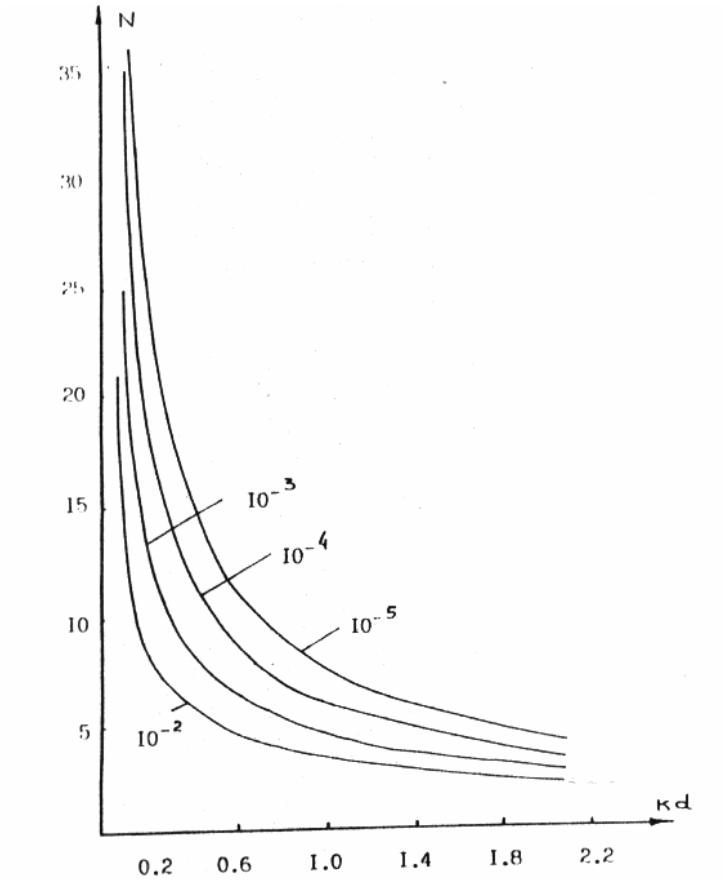

Figure 1.4: Dependence of the necessary number of terms (auxiliary sources) in summation (1.6) on the relative distance (along the normal) between the auxiliary and boundary surfaces for different precessions of the solution.

conditions are satisfied in a finite number of points located on two medium division surfaces.

$$\sum_{n=0}^{N} j_n \cdot WH_0(kR_{nm}) = Wf(X_m, Y_m) \quad n = 1,2,..,N; \quad m=1,2,..,M; \quad M>N \quad (1.13)$$

where: $R_{nm} = \sqrt{(X_m - X_n)^2 + (Y_m - Y_n)^2}$, W - is the operator of boundary condition and in case of perfectly conducted surface W=1 and in case of dielectric scatterer $W = \frac{\partial}{\partial n}$, n is the normal vector to the S surface.

It has been shown that the optimum approach is the Collocation Method, where the search of the amplitudes of auxiliary sources and their phases is reduced to the finding of the pseudo-solution of some over-defined (in general case) system of linear algebraic equations. Then this system has minimum size and simple matrix elements. If the number of collocation points equals to the number of sources, the boundary condition is satisfied exactly only in these points of collocation. If the number of collocation points is greater than the number of auxiliary sources the solution of the corresponding over-defined linear equations system is satisfied in the least square sense.

In contrast to other techniques, the collocation technique allows:

1. **To reduce the solution of the problem to the solution of a system of linear algebraic equations, which require minimal computer time.**
2. **To enable the solution of problems on the almost arbitrary, complex surfaces.**

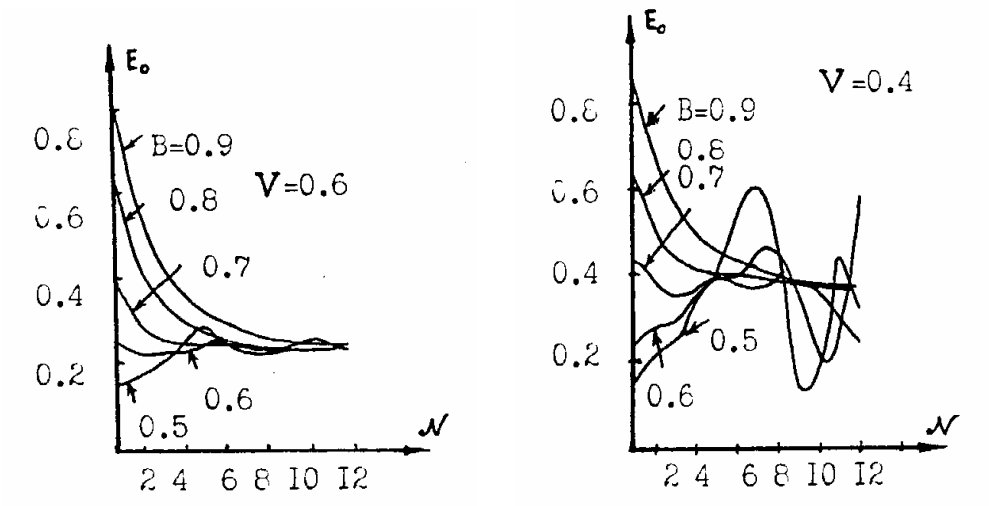

a) **b)**

Figure 1.5: Convergence of the E field amplitude in a fixed point versus the number of auxiliary sources. The problem investigated was the illumination of an conductive elliptical cylinder illuminated by plane wave. V stands for the ratio a/b while B stands for the ratio a_0/a where a_0, a are the radius of the auxiliary surface and cylinder respectively.

Notice that in the solution of systems of linear algebraic equations nothing will be changed if we replace the collocation points with source points and vice versa as it was observed by Waterman [13], named as - extended boundary conditions method. In other words, the auxiliary sources are kept on the surface of the conducting body and the collocation surface is shifted inside the body. Then the unknown coefficients are directly proportional to the current distribution along the surface of the body and the current distribution is obtained directly. This is the approach that was used to determine the current distribution on the scatterer surface. But implementation of the extended boundary conditions does not avoid the problem of Scattered Field Singularities consideration.

The method has some auxiliary parameters which are:

1. **The form and dimension of the auxiliary surface.**
2. **The procedure of distribution of the collocation points on the basic surface and the auxiliary sources on the auxiliary surface.**
3. **The number of the auxiliary sources.**
4. **The optimal choice of the enumerated parameters for the problem stated.**
5. **The evaluation of the calculation accuracy and its dependence on the auxiliary parameters.**

It was shown that the stability and convergence of the solution depend on the correct choice of the auxiliary parameters. In case of an incorrect choice of the parameters, the computing process might diverge.

Investigations have shown also that the correct choice of the auxiliary surface is very important to achieve efficiency. Consideration of the Scattered Field Singularities and the ‘resonance’ of the auxiliary surface is necessary.

The essential point is that the necessary number of terms of the mentioned series - Helmholtz equation's fundamental solutions, strongly depends on the relative distance (along the normal) between the real surface and the surface on which the auxiliary sources are placed. When the auxiliary surface moves away from the real one, the necessary number of the terms for calculation with the same accuracy sharply decreases and, consequently, computer time required decreases also (Fig. 1.4). This is the main idea of General Method of Auxiliary Sources.

The shift of the auxiliary surface is restricted by the location of the scattered field singularities because then results of calculation diverges as shown in fig. 1.5. Auxiliary surface should surround all singularities of the scattered field. Otherwise the Auxiliary Sources can not represent the scattered field entirely.

3. The General Algorithm Based on the MAS for Constructing the Solution of the Applied Electrodynamics Problems.

In this section the important recommendations are given for solution of applied electromagnetics problems by the Method of Auxiliary Sources in its general implementation when the special attention is not paid to the consideration of Scattered Field Singularities. Using these recommendations the great number of applied problems was solved and almost in all cases the desired accuracy was achieved with easy.

Long time experience has shown that the following recommendations should be taken into account during the solution of the problems by the Method of Auxiliary Sources.

a) For smooth surfaces the collocation points should be distributed uniformly;

b) The auxiliary surface should pass through the points which are located at the equal distance from the main surface, but not deeper than the minimum curvity radius;

c) Increase of the distance between the main and auxiliary surfaces improves the convergence. This distance should not exceed minimum radius of the negative curvature of the main surface;

d) In the case of edges at the main surface, it is more advantageous to smooth the edges under certain radius of curvature and to trace out its influence on the final results;

e) In diffraction problems on thin opened surfaces and screens the presence of some thickness of the order $\boldsymbol{kd=0.01}$ *should be assumed. It has been observed that the deviation from the true results does not exceed one percent.*

Taking into account these recommendations, the numerical results tend to the exact solution monotonically by increasing the number of collocation points. But in each specific case there are optimum values of the auxiliary parameters providing the desired accuracy.

However it is important to mention the significance of the major properties of scattered fields:

1. **The Scattered Field Singularities, and**
2. **The ‘resonance’ of the auxiliary surface.**

The knowledge of these problems allowed to increase the number of possible applications of MAS as well as the efficiency of the method. Investigations of the mentioned problems will be subject of the next section.

II. Problems, that Arise During the Numerical Implementation of MAS

1. Scattered Field Singularities

The fact that the analytically continued field must have the singularities in some area is proved by the following theorem [26]:

Theorem: *The analytical in the whole space solution of the wave equation* (1.1) *which satisfies the radiation condition and the boundary condition* (1.2) *on some surface for real k can be only identically equal to zero.*

An analytically described field, like a propagating wave, satisfies the radiation condition and carries the energy into infinity and must have the area of radiation (singularities) in some finite region. Otherwise it should be zero everywhere . A scattered field function is analytical everywhere outside the scatterer's surface. It has been shown, that if a current's magnitude and phase on the surface of the body are smooth, the scattered field can be continued analytically into the nonphysical area in the body up to the scattered field singularities that are located inside the scatterer.

The kind of singularities and their distribution depends not only on the geometry of scatterer, but also on the kind of incident field. The field reflected from an elliptical cylinder edge has phase centers located in the ellipse foci's region. Hence, the scattered field must have divergence near the ellipse foci. In the case of diffraction on the periodical structure [17, 22], the picture of equal-amplitude lines of the electric field when the lattice elements have elliptical section is shown in fig. 2.1. The depth of shifting of the auxiliary surface is restricted by the basic surface's foci (see fig.1.5) and the sources currents near the ellipse foci reach a large value and, practically, only these currents form the scattered field.

In a limited case, when the ellipse reduces to the strip, the above-mentioned singularity is known as "singularity of the edge". For an elliptical surface case this singularity is expressed weakly and they are located in the ellipse foci region. Thus, for better efficiency of the method the auxiliary sources must be located in the scattered field's singularity region, i.e. in convexity centers of the scattered field or in basic surface angles (in the case of a surface with edges).

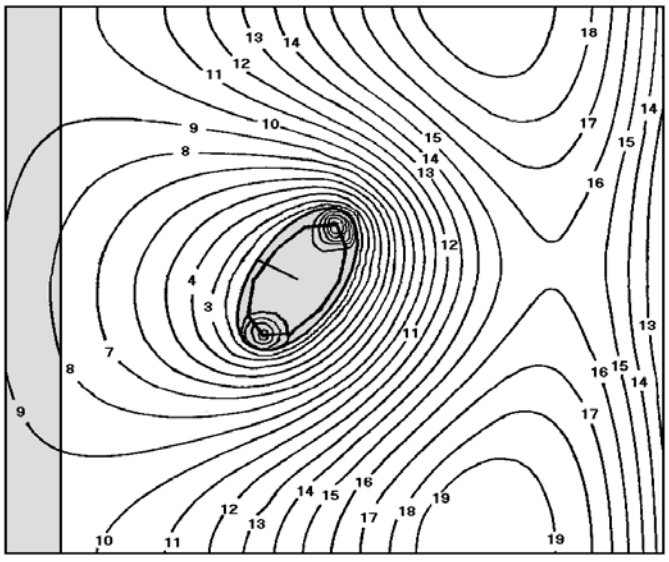

Figure 2.1: Metallic lattice over a layer of dielectric.

Scattered field singularities may arise because of the mirror image of incident field's singularity on the scattered surface. For simplicity let us consider the 2-D problem of the diffraction of linear source field like $-H_o^{(1)}(kr)$, located in distance $d_0 = -4$ units from a perfectly conducted infinite plane surface (Fig. 2.2a). The radiated field will have the following expression:

$$E^{inc} = H_o^{(1)}\left(k\sqrt{x^2 + (y - d_0)^2}\right).$$

The incident field will excite on the surface of the plate a current $J(x)$. It is evident that everywhere the current is parallel to the main linear source and it depends only on x coordinate. Following the classical integral equation method we divide the infinite plate in small patches of length dx, then each patch will radiate the scattered field like $H_o^{(1)}\left(k\sqrt{(x-x')^2 + y^2}\right)$, where $M(x,y)$ is the point of observation and x', is the patch coordinates. According to the method we have the following boundary condition on the infinite plate,

$$\int_{-\infty}^{\infty} J(x) H_0^{(1)}\left(k(x'-x)\right)dx = -H_0^{(1)}\left(k\sqrt{x'+d_0^2}\right) \quad (2.1)$$

where $J(x)$ is the unknown current distribution induced by incident field on the plate. Solution of this equation shows that the current distribution $J(x)$ will have a maximum in the point $M(0,0)$.

Now, let us shift the auxiliary sources line down at some distance d.

The maximum will increase and the values of the current in far points will decrease. In fig. 2.2b calculated values of the amplitudes of the distributed auxiliary sources are shown for

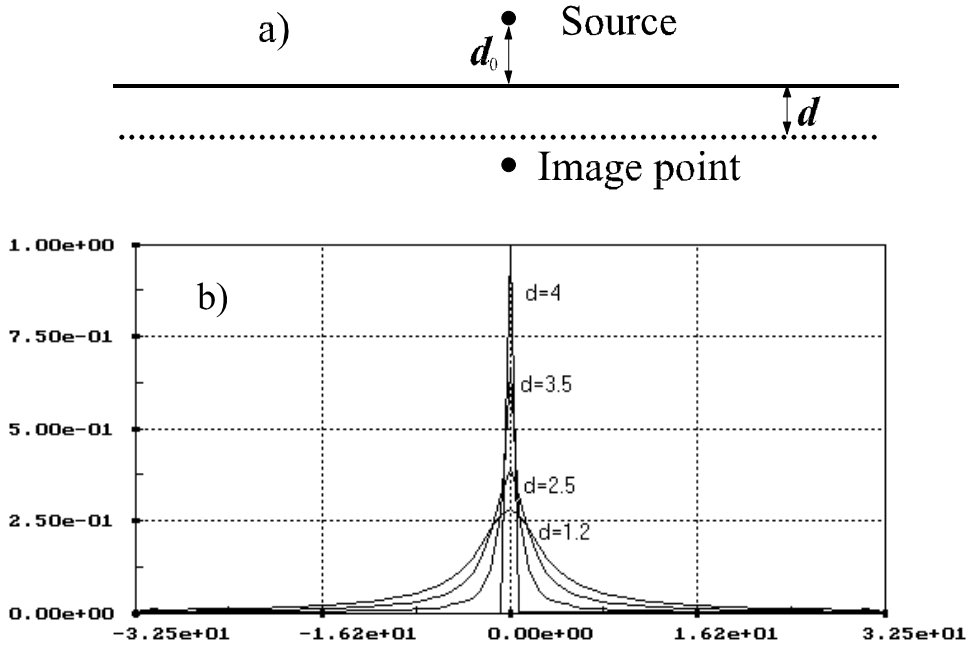

Figure 2.2: Calculated amplitudes of distributed Auxiliary Sources for different distances d

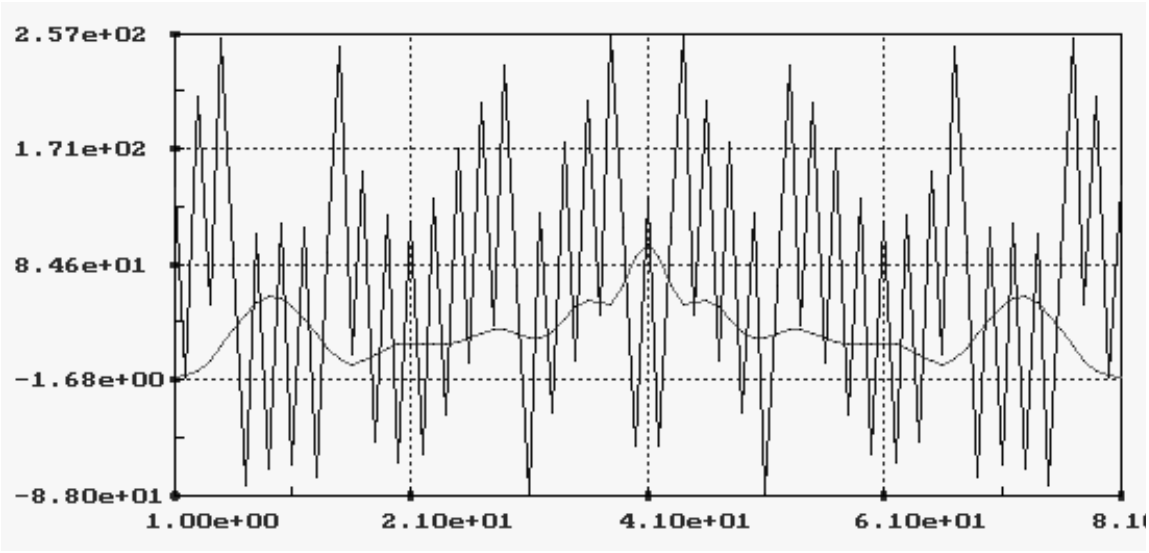

Figure 2.3: Amplitude and phases of Auxiliary sources for d=5

various $|d| < |d_0|$. If we continue this shifting until distance $-d_0$ (equal to the distance of the incident field source from the plate) only the current of the auxiliary source locating at the mirror image of the incident field source will be differ from zero. Its value will be equal to the incident field source value with negative sign. **Only one auxiliary source and one collocation point is needed for the fulfillment of the boundary conditions everywhere.** The point where this single auxiliary source is located is the point of singularity of the field scattered by infinite plane surface.

If we increase the distance of the auxiliary sources more than $|d_0|$, then the amplitudes of the auxiliary sources sharply increases, and their phases are not smooth. This is because none auxiliary source like $H_0^{(1)}$ distribution, situated further than the mirror image point can create a field that has its phase center in the mirror image point. In fig. 2.3 amplitude and phase distribution for auxiliary sources distributed at $d = 5$ are given (amplitudes takes high values and phase is rapidly changes). It is evident that the scattered field must have some kind of divergence center or area of energy divergence and corresponding scattered field's phase center which can not be created by $H_0^{(1)}(kr)$, situated further than the mirror image point. In the mathematical language it means that the system of functions $H_0^{(1)}(kr)$ distributed along a certain surface is not **complete** for representation of scattered field on the boundary surface when singularity is located between the auxiliary surface and the boundary surface. To this end the auxiliary sources that are used to describe the scattered field will create the high reactive field. This is the case when the system of auxiliary sources are not well chosen to create the mentioned scattered field. Using one linear source located in certain point the method becomes efficient because of the well known mirror image method results.

This example is very simple, indicative and didactic because for the case of linear source incident field and infinite plane surface the singularity is located in a single point.

Further in order to investigate: a) the variation of this singularity and how this single mirror image point is transformed into a caustic surface in case of optical region for more complex structures and main question b) is it possible to use elementary sources for efficient representation of any scattered field, the following examples will be studied:

1. Conductive cylinder illuminated by two symmetrically placed elementary sources.
2. Semi-infinite spaces with different permittivities.

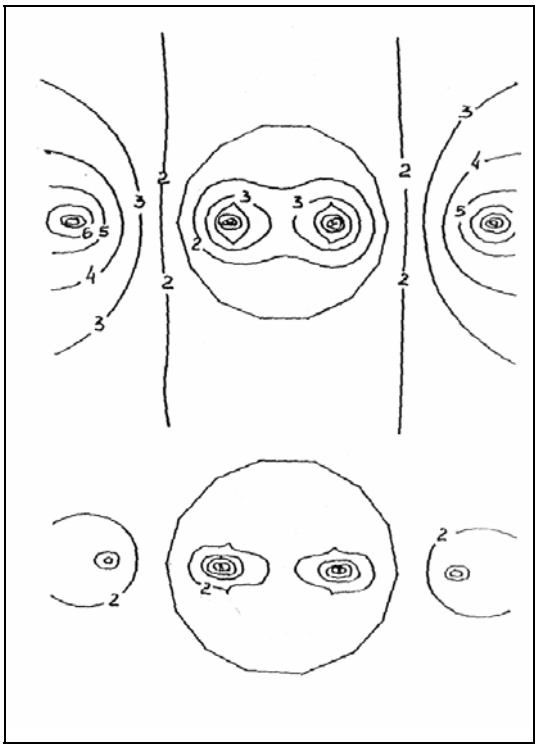

Figure 2.4: The equal amplitude lines of scattered field in case of two sources, located at small distance from circular cylinder.

3. Case 2 with the insertion of dielectric body in one of the two semi-infinite spaces.

4. Plane wave illuminating a conductive cylinder of big electrical radius. In these every separate cases dependence of Scattered Field Singularities (SFS) on the incident wave frequency will be investigated.

In the following attention is paid to the process of changing and replacement of SFS. It is important to examine the SFS of conductor plane transformation when the plane is rounded off to the cylinder or when the conductor is replaced by dielectric.

1. Consider the diffraction problem of two linear sources on a perfectly conducted cylindrical surface [17]. For $ka \approx 5$ two linear sources placed in right places provide accuracy of than 1% (fig. 2.4). The problem will be discussed later in more detail in section III

2. Consider the case of linear source in medium consisting of two semi infinite media with planar interface M_1 and M_2 of permittivities ε_1 and ε_2 respectively (see fig. 2.5). The incident field partly scatters in the plane border and partly is transmitted (refracted) in the second semi infinite space with the different permittivity. The exact solution of the problem is well known when the incident field is plane wave (calculated by Frensel's formulas of amplitudes and phases for reflected and refracted waves). The solution of this problem is also known when the incident field is linear source and is expressed with the use of Sommerfeld integrals. In applying the General MAS auxiliary sources are taken aligned inside the region 1 and 2 as shown in Fig. 2.5. The number of auxiliary sources used to

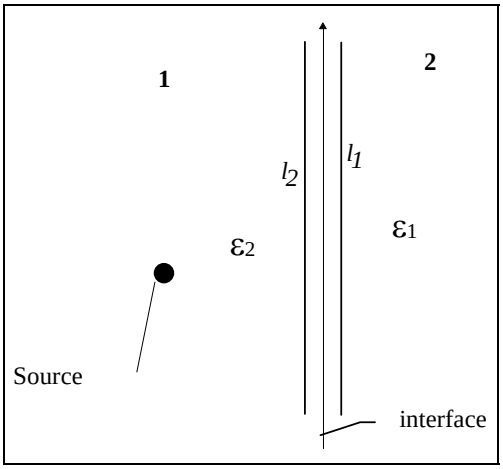

Figure 2.5: Geometry of the problem

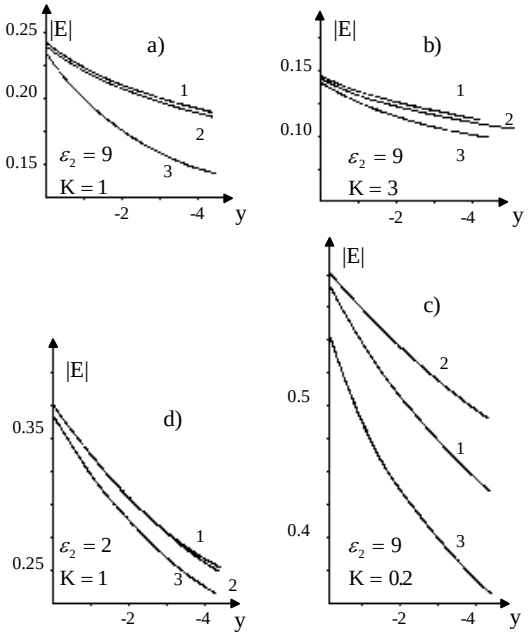

Figure 2.6: E- Field along y axis for different cases of *k* and ε, 1- exact solution, 2- auxiliary source located in optical image point and 3-auxiliary source located in electrostatic image point

describe the corresponding reflected (auxiliary sources inside region 2) and refracted (auxiliary sources inside region 1) waves determines the accuracy of the computation. However taking into account the fact that the refracted waves can be attributed to sources on the "caustic", semi infinite line:

$$x = -\frac{\left(n^2 - 1\right) \cdot x_0^3}{n^2 \cdot y_0^3} \quad (2.2)$$

$$y = \left(1 + \frac{\left(n^2 - 1\right) \cdot x_0^2}{n^2 \cdot y_0^2}\right) \cdot \sqrt{\left(n^2 - 1\right) \cdot x_0^2 + n^2 \cdot y_0^2} \quad (2.3)$$

as shown also in fig.2.7, the auxiliary sources can be taken optimally to achieve the fast convergence by using a single "image mirror point and few sources on the caustic line. In this context the equivalent sources associated with the electrostatic problem solution should also be considered. Indeed in case of electrostatics the boundary conditions on the $y = 0$ surface will be satisfied by selecting the equivalent sources at the points

$x = x_0$, $y = y_0 \frac{\varepsilon_2}{\varepsilon_1}$ - inside region 1

$x = x_0$, $y = -y_0$ - inside region 2

while in optical frequencies the boundary conditions on the $y = 0$ surface will be satisfied by selecting the equivalent sources at the points:

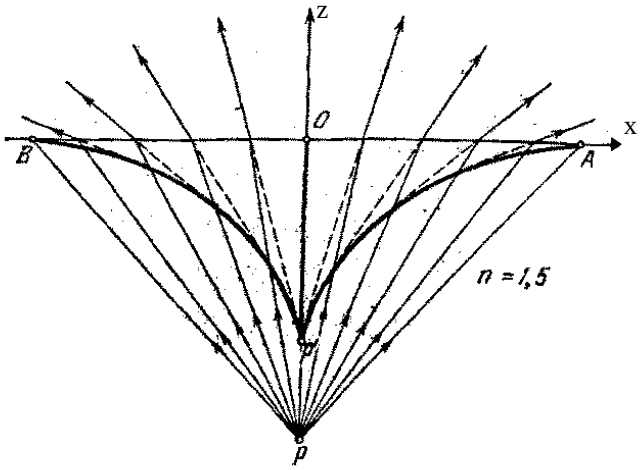

Figure 2.7: Caustic surface for meridian rays.

$x = x_0, y = \sqrt{\varepsilon_2 / \varepsilon_1}\, y_0$ - inside region 1

$x = x_0, y = -y_0$ - inside region 2

In fig.2.6 comparisons of computed results for the refracted field along the axis (x_0, y) using for the representation of the refracted field by an auxiliary source placed in the optical image point (curve 2), in the electrostatic image point (curve 3) and the exact solutions (curve 1) are given.

The analysis of these graphics shows that it is necessary to locate the auxiliary source in the optical image point which takes into account the phase centre of the refracted field [19].

To solve this problem let us remind the concept of caustic surface. At the situation in which there is the point source *P* in dielectric of higher refractive index than where observer is located, the interface between the two being a plane (fig. 2.7). It is well known from geometric optics that the image appears in the place where nearby rays focus, i.e. on the caustic of the refracted rays (fig. 2.7). The line along which an observer sees the image is tangent to the caustic. So the apparent location of the sources depends upon the position of the observer and its apparent direction from the observer will not be that of the true source except at normal incidence.

The fig. 2.8 shows the caustics in two cases. The first one is when the source is placed in dense medium and the second is when the source is placed in light medium.

In the conventional method of auxiliary sources, where we do not consider the SFS, the approximate solution of the near field calculation problem will be obtained as follows. Two surfaces of auxiliary sources, first left and the second right of the border, will be introduced, in order to calculate the scattered and the transmitted fields respectively. Fulfillment of the boundary conditions in the border will determine the amplitudes and the phases of the auxiliary sources introduced before. The solution of the problem with this distribution of auxiliary sources will then be achieved and the computational error will depend on the number of auxiliary sources used. Then, if the field singularities are considered using the knowledge of the existing caustic surface of the refracted field, the solution of the problem should be computational improved.

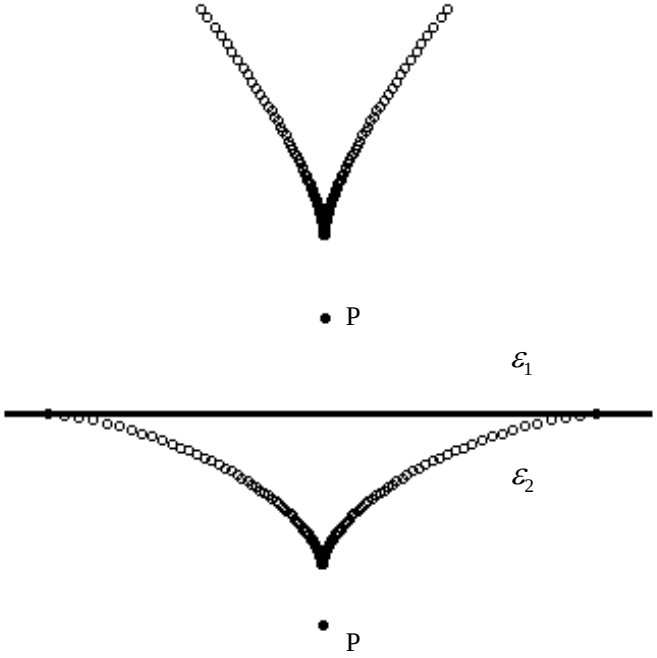

Figure 2.8: Caustic surface for meridian rays.

3. Let us now complicate the last problem with the insertion of a body, with permittivity ε_1 near the border of two semi-infinite spaces with permittivities, first ε_2 and second ε_3. Assume also that the incident field is induced by the linear source situated in the second semi-infinite space, while the dielectric body is placed in the first semi-infinite space. The conventional method of auxiliary sources assumes auxiliary sources distributed in both sides of the semi-infinite-planes border $l_2^{'}$ and l_3 respectively and additional auxiliary sources are distributed inside l_1 and outside l_2 the body surface.

The auxiliary sources in the surface l_3 are used to describe the scattered field by the border of the two semi-infinite spaces, the auxiliary sources in surface $l_2^{'}$ are used to describe the transmitted field in the dielectric area ε_2, the auxiliary sources in l_1 are used to describe

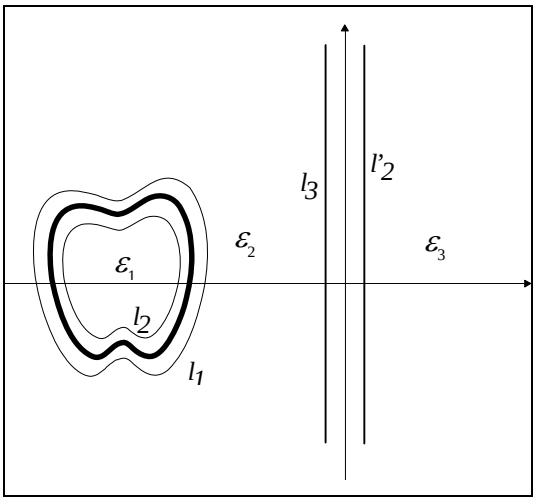

Figure 2.9: Geometry of the problem in conventional MAS.

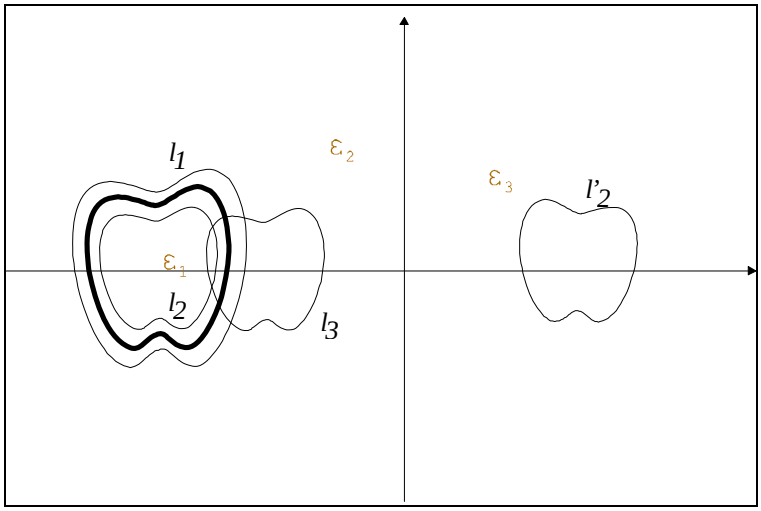

Figure 2.10: Geometry of the problem, using scattered field singularities.

the field induced inside the dielectric body and finally the auxiliary-sources distributed in surface l_2 describes the scattered by the dielectric body field.

The amplitudes and phases of the auxiliary sources will be determined during the fulfillment of boundary conditions *E*, and *H* fields in the dielectric borders. The solution of the problem stated bellow is achieved, and compared with the solution given when we consider the existence of the field singularities.

In fig. 2.10 a more efficient way to distribute the auxiliary sources is shown.. The results obtained using this auxiliary source's distribution are better by the meaning of higher accuracy with less number of auxiliary sources. The number of the sources used in surfaces $l_2^{'}$ and l_3 is decreased but also the number of collocations points in the semi-infinite spaces border is decreased. The reason is that when we put the auxiliary sources in the field singularities positions the boundary conditions tend to be fulfilled in a greater area than we demand fulfillment. As in the example of the diffraction problem of the linear source by an infinite perfectly conducted plate, one collocation point is needed to fulfill boundary conditions on the metal surface. Same situation is met in this problem, so the methods convergence is very high with respect of the boundary conditions in the semi spaces border. The fulfillment of the boundary conditions in the far points of the border is obtained just by demanding the fulfillment of the boundary conditions in the near points of the border. For situation where distance between interface and dielectric body is a few wavelength and for $ka \approx 10$ the calculation time is a few seconds. The approach described above was implemented for the calculation of various problems as shown in figures 2.11 (a), 2.11 (b), 2.11 (c). The results of investigations of these problems gave the characteristics the near field for excitation of dielectric bodies located near the border of two semi-infinite dielectric spaces. The resonance disturbance of the near field was obtained, that depends on the size and permittivity of the body and the characteristics of the nearby media. This disturbance allows to identify the inserted body with known electrodynamic parameters [19].

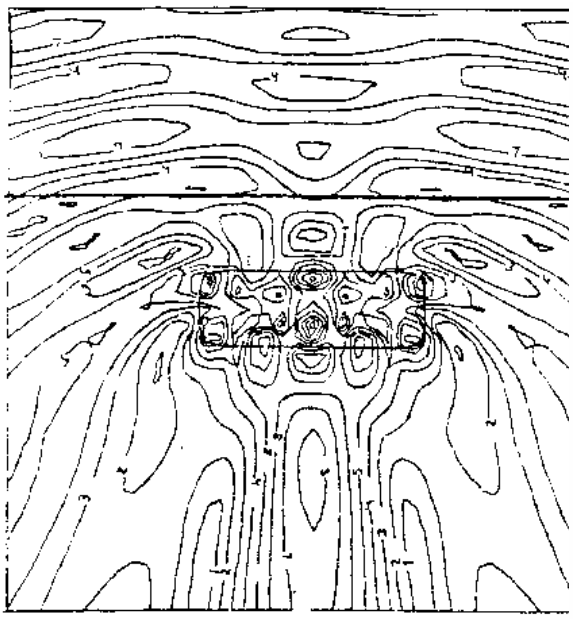

Figure 2.11 (a): The inserted body

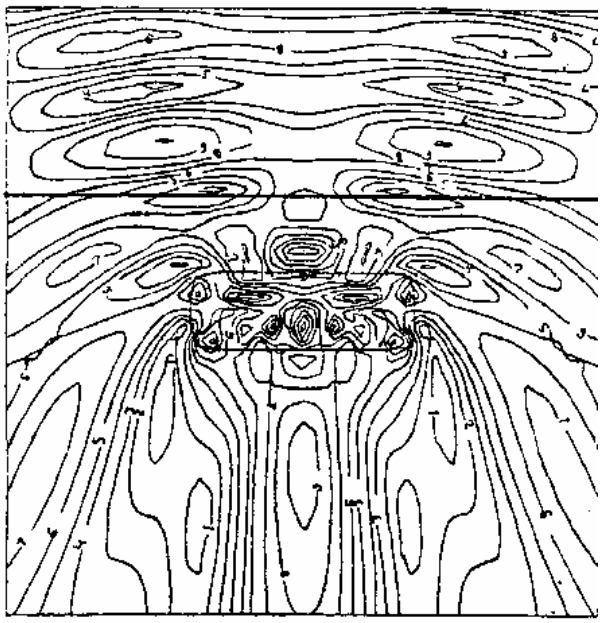

Figure 2.11 (b): The inserted body

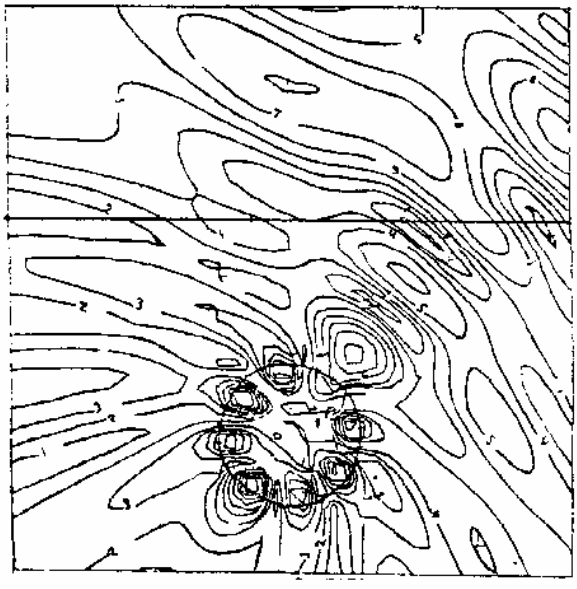

Figure 2.11 (c): The inserted dielectric cylinder

4. In the case of the perfectly conducting cylinder illuminated by the plane wave or linear source the singularities are distributed along the caustic like the bright points with the distance between them depended on frequency (fig. 3.10). The investigation of this distribution needs the special consideration. This was done with the help of visualization method presented below. For this reason the solution of mentioned problem is given in Section III.

From the above discussion it is clear that the Scattered Field Singularities always exist and their consideration improves the convergence and accuracy of solution.

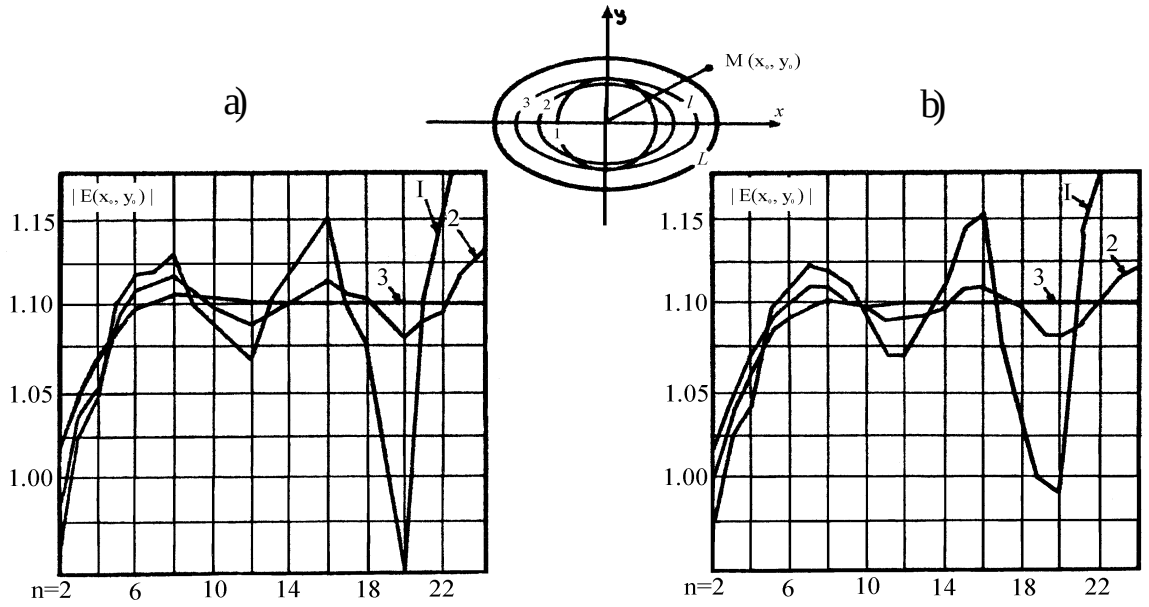

Fig. 2.12: Convergence of solution in case of (a) collocation and (b) extended boundary conditions methods.

One can be not correct to assume that the usage of extended boundary conditions can avoid the consideration of Scattered Field Singularities. On the fig. 2.12 (a, b) the dependence of convergence on the geometry of auxiliary surface in two cases is shown: with the collocation method and with the method of extended boundary conditions. It is seen that only for the curve 3 when both the auxiliary and extended boundary surface contains the singularity the convergence occurs. And in both cases when the singularity is outside of these surfaces the solution diverges.

The essential is that the usage of the shifted auxiliary sources (or Method of Auxiliary Sources) as well as the extended boundary conditions methods assume as the basic idea that the scattered field can be analytically continued inside the scatterer's surface. And in both cases this auxiliary surfaces can be shifted up to the singularities of scattered field.

The same is true for the expansion (1.7) for which the convergence is circular. And in this case also the expansion (1.7) can be used until the area where the expansion (1.7) diverges contains all Scattered Filed Singularities and is completely located inside the scatterer.

These problems are related to "Relays hypothesis" and discussed in [18, 20].

Another problem in solution of electrodynamics problems by the MAS arise due to the resonance of the auxiliary surface. The discussion of this follows next.

2. The "Resonance" of the Auxiliary Surface (Solution of Interior Problems)

During the solution of diffraction problems it has been noted that for some critical values of wavenumber k_a (for example in case of circular cylinder) convergence becomes worse and problematic [30,31]. Investigation has shown that the "critical" values of k exactly coincide with the eigenvalue of the region bounded by the auxiliary surface. At the same time, the fields inside the auxiliary surface describe the eigenfields of the region. Similar patterns of the eigenfields are observed inside the basic surface if the auxiliary surface is out of the region D.

During more detailed investigation [32,33] it has been shown that these k_a with high accuracy were in agreement with eigenvalue of inner area. Unlike the other values of k, penetration of electromagnetic field into the inner area is observed, and this field is exactly the eigenfield of the inner surface. That is the reason for sharply changing field values around k_{res}. Results will not be changed in the case of using shifting boundary conditions.

Consider the problem of calculation of eigenvalues and eigenfields of the along - regular waveguide. Usually, such problems are reduced to the solution of a system of homogeneous algebraic equations and further a set of parameters is determined for which this homogeneous system possesses a non trivial solution. As it is known, the process of investigation of the dispersion properties of various waveguide systems includes the calculation of propagation constants, impedance, losses etc. This requires the calculation of eigenmodes with large accuracy. Therefore the conventional methods based on a solution of a homogeneous system, in a numerical realization meets difficulties which become insuperable for high mode of fluctuations.

Firstly - the determinant of a corresponding homogeneous system becomes close to zero in a wide range of parameters and then the search of critical values of the parameters is difficult. Secondly - the process of computation account of eigenmodes is formidable. The error of calculation grows sharply for high order of modes.

Such problems are met even in the case of a simple propagation along regular hollow metal waveguide. The problem becomes even more complicated in the case of dielectric waveguide. On the basis of MAS, a relatively simple method for eigenmode calculations is suggested [32,33]. The then problem is reduced to the solution of a non- homogeneous system of linear algebraic equations.

Consider the solution of two-dimensional scattering problem on the basis the Fredholm singular integral equations of the first kind [26] and assume that a monochromatic electromagnetic wave incidents a perfectly conducting cylindrical body with cross section surface L. Then, the determination of diffraction field is reduced to the solution of boundary problem (1.2, 1.2) in which the operator W - is either the unit operator (E - polarization), or the derivative along the normal to the surface L (H - polarization).

If the solution of the problem is formed as the determination of the currents induced on the surface L as follows:

$$U(x,y)=\int_L J(L)H_0^{(1)}\left(k\sqrt{(x-x_1)^2+(y-y_1)^2}\right)dL\,, \quad (2.4)$$

then the problem is reduced to the solution of the following Fredholm singular integral equation of the first kind:

$$\int_L J(L)H_0^{(1)}(k\sqrt{(x^*-x_L)^2+(y^*-y_L)^2})dL = E_z^i(x^*,y^*), \quad M(x^*,y^*)\in L. \quad (2.5)$$

As is known, the given problem is incorrect according Hadamard. Furthermore, a solution may not exist for any right hand side of (2.5).

Despite Hadamard's restrictions, in those problems of diffraction which are reduced to the solution of the given integral equation, the mentioned incorrectness does not manifest itself. Firstly in the problems of diffraction, more often, we are interested not in the currents but in a scattered field, in which the rapidly oscillating term $i(L)$ of the current does not change the result:

$$\int_L i(L)H_0^{(1)}(k\sqrt{(x-x_L)^2+(y-y_L)^2})dL \approx 0. \quad (2.6)$$

Secondly, the right hand side of (2.5) in all practically important problems of diffraction is a smooth function on the surface L, which itself is a solution of (1.1) and guarantees the existence of the solutions of the boundary problem (1.1, 1.2) and of the integral equation (2.5). This is confirmed by many authors [35, 42, 43] where the two-dimensional and three-dimensional scattering problems are solved using Fredholm singular integral equations of the first kind.

From the above considerations a number of important conclusions derives as follows: the function, determined by formula (2.4), coincides with an incident field $E_z^i(x,y)$ not only on the boundary of the area *D*, but also everywhere inside *D*.

$$\int_L J(L)H_0^{(1)}(k\sqrt{(x_l-x_L)^2+(y_l-y_L)^2})dL = E_z^i(x_l,y_l), \quad M(x_l,y_l)\in D,, \quad (2.7)$$

where *J(L)* is the solution of the integral equation (2.5). The functional relation of *J(L)* (2.7), in the method of "shifted boundary conditions" [13], is considered as a non-singular integral equation.

We consider some properties of the solution of this equation: a) The integral equations (2.5) and (2.7) have the same solutions; b) If the wave number k coincides the eigenvalue k_i of the Dirichlet's or Neumann's problem for the area D_0 bounded by surface l, then the solution of a equation (2.7) consists of two terms

$$J_0(L) = J(L) + \omega_i(L), \quad (2.8)$$

where $J_0(L)$ is the solution of (2.7); $J(L)$ is the solution of (12.5); $\omega_i(L)$ - is a nontrivial solution of homogeneous integral equation:

$$\int_L \omega_i(L)H_0^{(1)}(k_i\sqrt{(x_l-x_L)^2+(y_l-y_L)^2})dL = 0. \quad (2.9)$$

Then follows that the eigenfield of the area D_0, for the wave numbers k_i is formed as:

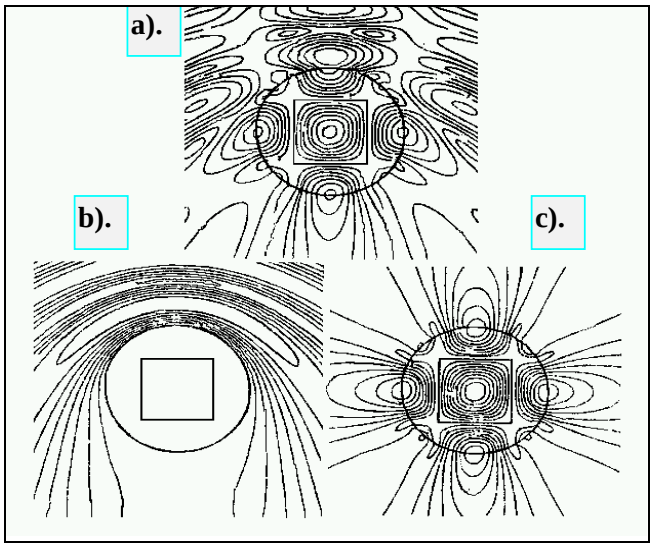

Figure 2.13: Fields in the near zone of the cylinder.

$$U_i(x,y) = \int_L J(L) H_0^{(1)}(k_i \sqrt{(x-x_L)^2 + (y-y_L)^2}) dL - E_z^i(x,y) \quad (2.10)$$

Actually the first term of (2.8) provides compensation of the incident $U_i(x,y)$ everywhere in the area **D** (fig. 1.1) (since it is the solution of (2.5)) , and the second term $\omega_i(L)$, as the eigencurrent, describes an eigenfield in this area. Numerical results for the problem of a rectangular waveguide illuminated by plane wave are shown in fig. 2.13. The auxiliary surface is a circle of radius $a = 1$. The collocation points are located at the square of size $l = a$. The integral equation (2.7) is numerically solved for wave number $ka = \sqrt{2}$, which is critical for the square. fig. 2.13(a) is the superposition of the diffraction field, shown in fig. 2.13(b) and the eigen-field of the square, shown in fig. 2.13(c).

Therefore, investigations have shown that these *ka* with high accuracy were in agreement with eigenvalue of the inner area. Unlike the other values of k the penetration of electromagnetic field into the inner area is observed and the distribution of this field is exactly the eigenfield of the inner surface. That is the reason for sharply changing field values for k_{res}.

When $k = k_{res}$ the solution of the homogeneous system of linear equations superimposes on the solution of an nonhomogeneous system of linear equations of diffraction problem.

$$\sum J_d H_0^{(1)}(kr(x_{m,n}, y_{m,n})) = U^i(x_m, x_n)$$

$$\sum J_{res} H_0^{(1)}(kr(x_{m,n}, y_{m,n})) = 0 \qquad J_{tot} = J_d + J_{res}$$

Similar: $U(x,y)=U_1(x,y)+U_2(x,y)$. Fig. 2.13 shows the field in the near zone. The part of the incident field penetrate into and for the resonance frequency of the square excited oscillations. For $k=k_{res}$ the field of the eigencurrent creates the eigenfield that penetrates everywhere and superimposes on the diffraction field.

Using the properties of the integral equation (2.7) a simple algorithm for calculation of critical frequencies and eigenfields of the along-regular metal and dielectric waveguides is derived.

Such algorithm was used for the solution of several interior problems. Solution of a great number of applied problems of this kind has shown that this method allows the calculation of eigenmodes with high accuracy. Additional calculation of high wave oscillation modes does not require extra accuracy or supplementary auxiliary sources. Accuracy of calculation of all modes is the same in contradiction with the 'traditional' methods of solution of homogeneous equations where high order calculations, requires much more numerical cost.

Therefore, according MAS, there is a deep relation between diffraction and eigenvalue problems, and this gives the possibility of investigating them almost simultaneously using same methods and algorithms. To avoid the resonance phenomena during the diffraction problem solution it is enough to demand the total field to be zero in particular point inside the investigated area.

The present method for the solution interior problems must be considered as a mathematical model of the physical experiment in which resonant frequencies and eigenfields of the resonator are determined from the condition of the field's sharp increases in the internal region with the radiation of the system by changing the field's frequency.

Eigenfgield's singularities are created and determined only by the main investigated surface and they are located in concavity centers in fracture points of the studied surface (fig. 2.14).

The presented method of calculations based on the solution of an inhomogeneous system of linear algebraic equations allows one to determine more precisely the eigenvalues, simplifies the calculations of the eigenfunctions, and does not require any additional

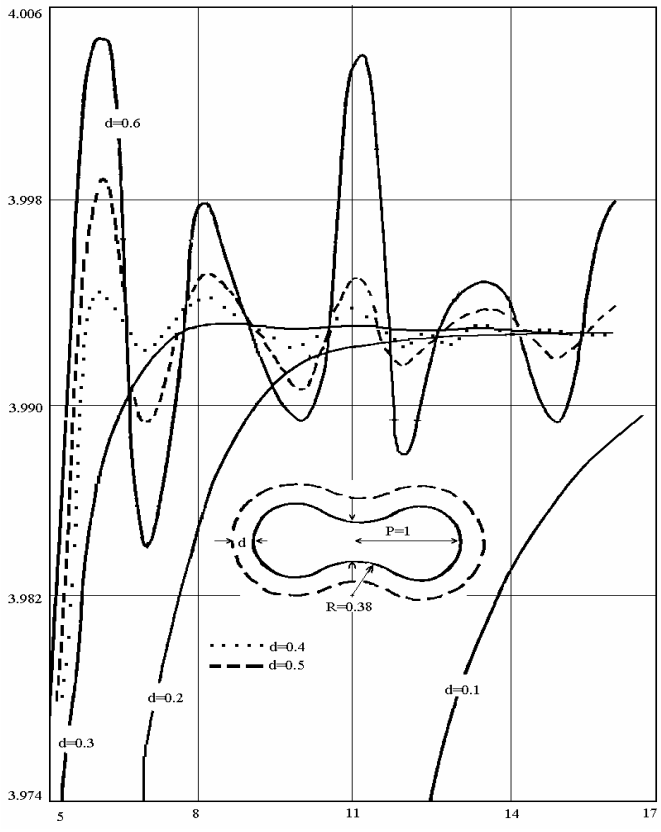

Figure 2.14: Dependence of convergence from the form of auxiliary surface. Minimum radius of curvature of a main surface $R_{\min} = 0.38$**. For a distance between the surfaces** $d > R_{\min}$ **results diverges**

increasing of N for computing supreme modes. As an example the solution of particular problem of regular metal waveguide is given. The same approach is applied to the dielectric waveguides.

The investigation of along-regular hollow metal waveguide.

As is known, the investigation of dispersion properties and eigenfields at the along-regular waveguides is reduced to the solution of the following homogeneous boundary problem for the Helmholtz equation. Let us find in the area D_0, bounded by the surface l, a non trivial solution of the equation

$$\Delta U(x,y)+g^2U(x,y)=0, \quad (2.11)$$

which satisfies the boundary condition

$$WU(x,y)=0; \qquad M(x,y)\in l, \quad (2.12)$$

on the surface l, and the spectrum $\{g_i\}$ of those values of the parameter g, for which these solutions exist.

The algorithm of calculation of critical frequencies and eigenfields consists in the following [33]:

a) Let the collocation points $\{x_m, y_m\}$, (m=1,2,..., N) be placed on the main surface l;

b) Let us construct such an auxiliary surface L, which completely surrounds the main area D_0, and distribute on it the N centers of approximation $\{x_n, y_n\}$, (n=1,2,...,N);

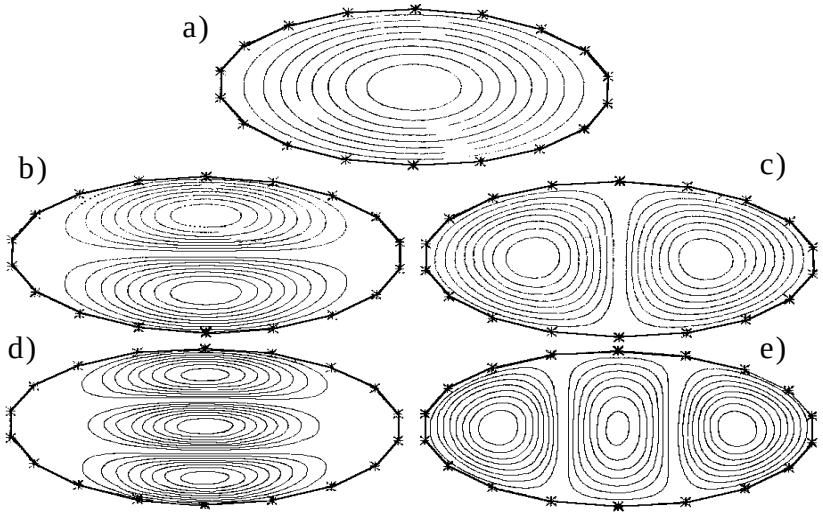

Figure 2.15: Eigenfields of elliptic waveguide $a/b = 0.5$**:**
a) Wave of a type E_{01}, $\lambda/b = 1.68$**;**
b-c) Wave of a type E_{02}, $\lambda/b = 0.91$, $\lambda/b = 1.25$**;**
d-e) Wave of a type E_{03}, $\lambda/b = 0.63$, $\lambda/b = 0.99$.

c) Define the auxiliary function $U_i(x,y)$, as some known, particular solution of the boundary problems (2.11-2.12) (for instance, the function describing the field of the linear source, located outside of the area D_0);
d) Rewrite the integral equation corresponding to the boundary condition (2.12) in the equivalent form of the system of linear algebraic equations:

$$\sum_{n=1}^{N} J_n \; WH_0^{(1)}\left(g\sqrt{(x_n - x_m)^2 + (y_n - y_m)^2}\;\right) = WU^i(x_m, y_m) \quad (2.13)$$

e) Solve the system (2.13) for various values of the parameter g and trace out the behavior of the function:

$$U(x_0, y_0) = \sum_{n=1}^{N} J_n \; WH_0^{(1)}\left(g\sqrt{(x_n - x_0)^2 + (y_n - y_0)^2}\;\right) - U^i(x_0, y_0) \quad (2.14)$$

in some point $M(x_0, y_0)$ of the area D_0. Find those values of the parameter g for which this function reaches its relative maximum.

Just these values of the parameter g will correspond to the eigenvalues of the given area, and the function (2.14) for these g will describe the eigenfied (fig. 2.15). For a given case five auxiliary sources and five points of a collocation provide accuracy of calculation on the order of 0.1 % (taking into account symmetry).

Similar method have been used for calculation of dispersion characteristics of dielectric waveguides as well as planar waveguides [33].

III. MAS for Field Visualization and Scattered Field Singularities

1. The General Algorithm Based on the MAS for Field Visualization

The previously mentioned examples proved that the knowledge of Scattered Field Singularities location is important. One of the best method for Scattered Field Singularities localization is to reconstruct the scattered field up to its sources - singularities. There are many methods for reconstruction of the analytical continuation of wave fields. Mathematical justification of the suggested approach is given in [34,35]. There are also some other known attempts to realize the idea of microwave fields visualization presented in [36]. In the present chapter the holographic method of wave fields reconstruction by known data of scattered fields amplitudes and phase on some surface in approachable area is implemented. The method suggested here is based also on the Method of Auxiliary Sources. In the MAS the scattered wave field is efficiently determined and reconstructed using a number of functions, describing propagating waves, by forcing fulfillment of boundary conditions on the scatterer's surface. The new idea of using functions describing the field which energy comes to them is introduced in this article. Such function is the $H_0^{(2)}(kr)$ in 2-D problems.

Let us now assume a body scatterer (fig. 3.1), illuminated by some incident field induced by a source at the point (x_0,y_0). Then assume that in a certain surface *S* on some distance from the object, the complex scattered field $U^s(x,y,z)\big|_S$ is known (amplitude and phase). The aim is to reconstruct the scattered field around the object up to its singularities (sources of scattered fields or re-emitters). To this end on the surface *l*, near the surface where the field data are known, auxiliary sources with the same frequency are distributed. It is of great importance to determine the type of sources used in the auxiliary sources distribution. Since the auxiliary sources will be used to describe the field coming to them, the phase velocity of the scattered field should be pointed to this sources. Thus it is certainly needed to use appropriate sources on the surface, which will behave as absorbers, creating a field that comes to them.

$$\sum_{n=1}^{N} a_n H_0^{(2)}(kr_n) \quad (3.1)$$

Then the known scattered fields is tied up with the field of Auxiliary Absorbers. The systems of linear equations derived is described as:

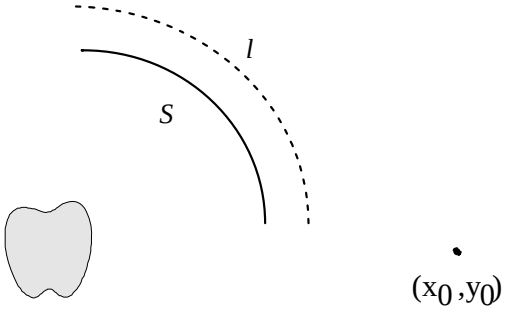

Figure 3.1: Singularities visualization method.

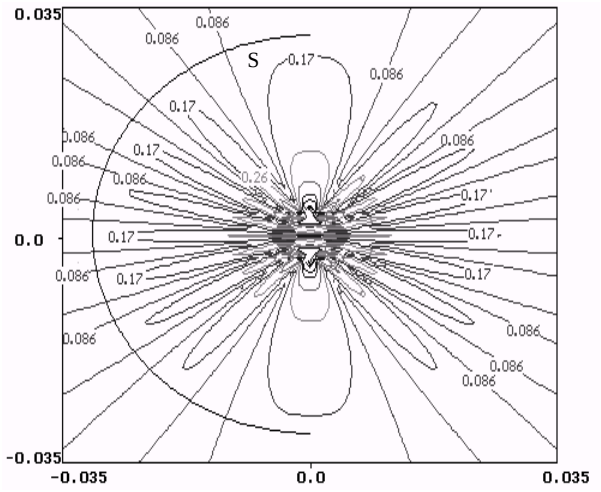

Figure 3.2: Field radiated by the two sources

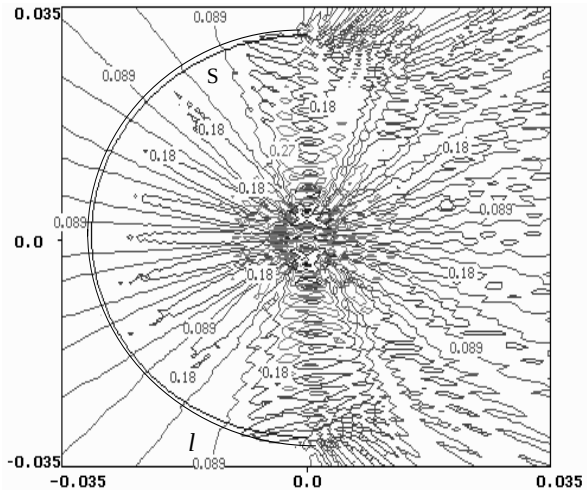

Figure 3.3: Reconstructed field

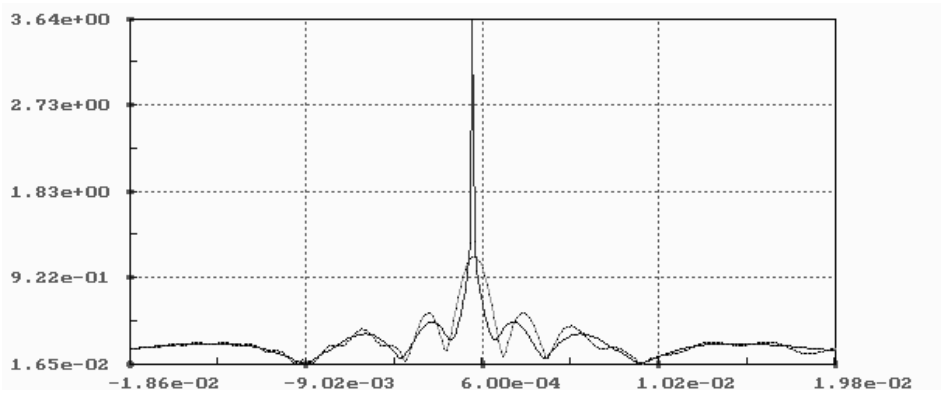

Figure 3.4: Real and reconstructed field for y=4mm

$$\sum_{n=1}^{N} a_n H_0^{(2)}(kr_{nm}) = E(r_m) \quad (3.2)$$

This allows to find out the amplitudes and phases of Auxiliary Absorbers by solution of the corresponding system of linear equations (3.2).

Because of the uniqueness of analytical continuation of wave field, the field of auxiliary absorbers will restore the field up to the main singularities into the non-physical area of the metallic object. In the case of semi transparent objects the method introduced will restore the main scattered field singularities inside the body.

2. The Validation of the Algorithm for Field Visualization

a) Numerical Results

To give an example of how the method works lets consider two sources in the 2-D space at positions (0mm,4mm) and (0mm,-4mm) [37]. The near field distribution of these sources with $\lambda = 2\text{mm}$ is illustrated in fig. 3.2. Next, the calculated amplitudes and phases of this field on a certain curve S of radius 31mm, also shown in the figure, are recorded. Then, according to the described above algorithm, auxiliary absorbers are distributed on the

auxiliary surface *l* (fig. 3.1) and the amplitudes and phases of the auxiliary absorbers are determined by tiding the field radiating from them with the field already known on the curve S. In fig. 3.3 the field reconstructed by the auxiliary absorbers is presented. It is shown that the field radiated from the auxiliary sources has two maximums at the coordinates of the initial radiating sources, thus the method allows to determine the coordinates of the elementary radiating sources. Also, in fig. 3.4 both real and reconstructed fields for y=4mm are shown. The accuracy of the field reconstruction up to the scattered field singularities along the *x*-axis is within several percent.

b) Experimental Results

To proof this concept the experiment was carried out to reconstruct the Scattered Field from the, conductive cylinder illuminated by some EM field source [37]. The scattered field amplitudes and phases are measured and recorded on a line *S* at the far field region, as shown in fig 3.5. Then, on the outer side of *S*, auxiliary "absorbing"-sources are distributed and their amplitudes and phases are selected to reconstruct the scattered field distribution on *S*. In fig. 3.5, the scheme for field measuring and reconstruction using the measurements results is shown for a metallic cylinder. For the implementation of the experiment as source generator was used the HP8510C Vector Network Analyzer with a frequency range up to 50GHz and power 5dBm. A horn antenna was used to illuminate a 60cm height, large compared to the wavelength, conductive cylinder placed in center. The size of pickup moving along the half circle was about 0.8mm. The frequency used was 30GHz cm while the radius of the cylinder was 2cm. The observation half circle *S*, shown on the left picture (fig. 3.5), is of radius 30cm. The mentioned equipment allows to measure the amplitude and phase of electromagnetic field. The measured data were used then to reconstruct the analytical continuation of the wave field by the method described above (right picture). From the obtained results it is evident that the method enables to localize the Scattered Field Singularities inside the scatterer and thus provides an efficient and highly simple target imaging technique.

The distinct property of the described reconstruction method is that the result of visualization does not change if the field of other sources placed outside the region between the object and visualization area is added to the measured values. This is true as for any holographic methods where these undesirable sources do not change the whole obtained picture.

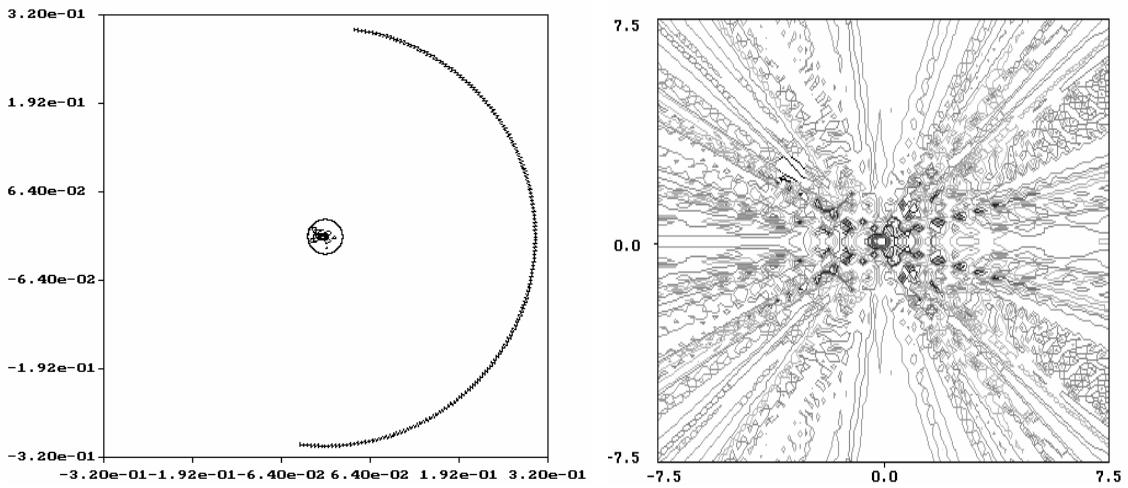

Figure 3.5: Reconstructed field for a cylinder of 2cm diameter

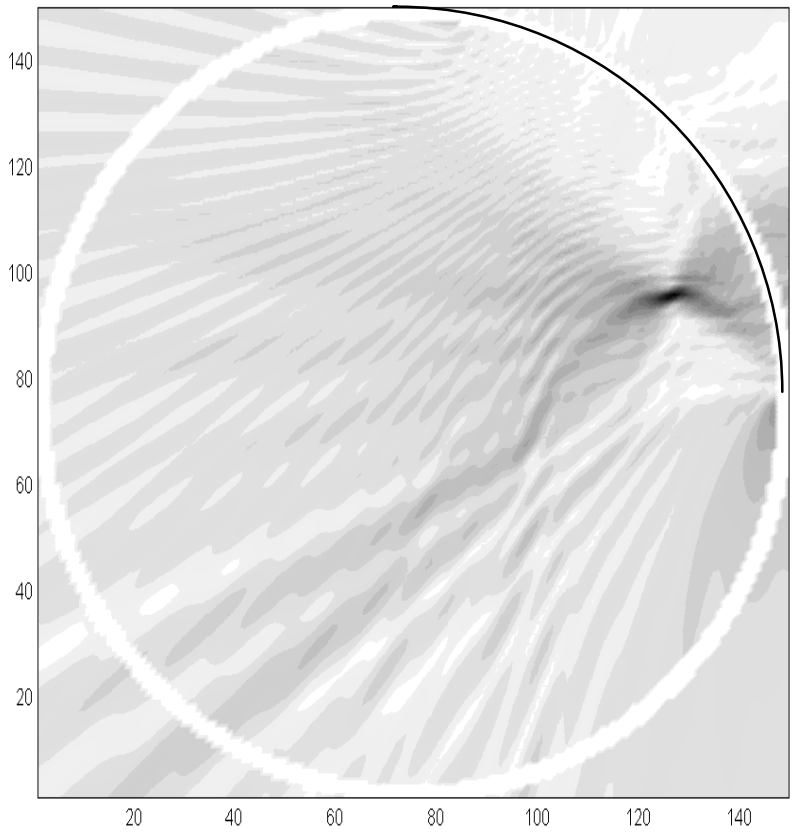

Figure 3.6: The amplitude distribution of the reconstructed field (black arc corresponds to the points were the scattered field was measured in experiment)

The same reconstruction algorithm is also valid for imaging purposes using an ultrasonic waves. The corresponding experiments was carried out also in Technical University of Athens. A dielectric cylinder was placed in the tank filled with water. This cylinder was illuminated by an ultrasonic source at the frequency of 50 kHz and the scattered field was measured at some distance from the cylinder on the arc. The sensor with narrow pattern (less than 2^0) was used as receiver for field measurement. Then, applying the described above algorithm, the measured data ware used for field reconstruction in the region were the cylinder was placed. Fig. 3.6 shows the amplitude distribution of the reconstructed field. The dark area corresponds to the highest value of the reconstructed filed and points to the place were the original scatterer (dielectric cylinder) was placed.

The described above experiment demonstrates that the proposed reconstruction algorithm can be applied for ultrasonic waves too and offers the possibility for simple ultrasonic imaging.

3. Visualization of Scattered Field Singularities

Following the method described before for the localization of the scattered field singularities, two problems, (not discussed in detail in previous paragraphs) will be considered. In the first problem a conductive cylinder illuminated by two sources symmetrically placed very close to the cylinder surface is considered. According to the scattered field visualization method the higher valued singularity points are determined. The idea is to distribute auxiliary sources in these maximums with the amplitude and phase of the reconstructed field in order to form the scattered field. In fig. 3.6(a) only two auxiliary sources symmetrically placed are located in the scattered field singularities points. It is shown that even for high $ka = 64$ consideration of the singularity points helps, by mean of giving to the scattered field the curvity of the cylinder, fig. 3.6(b) four sources are used again placed in the main scattered field singularities points and the improvement is obvious. Note in fig. 3.6(a). and 3.6(b). the improvement of the scattered field diagram, by the mean of fulfillment of the boundary conditions (In fig. 3.6a. low levels of field are not shown).

Also in fig. 3.7 and fig. 3.8 comparison between the solutions given by conventional MAS and MAS considering Scattered Field Singularities is made. In fig. 3.7a. the total field in a sector of 20 degrees at distance 0.039, (incident field source located at ±0.036, cylinder radius 0.03, wavelength 0.003) is shown. In detail line i represents the total field using 250 auxiliary sources in conventional MAS, were the accuracy for the scattered field was better that 0.1%, line ii represents the scattered field calculated with twelve sources located on the scattered field singularities positions and line iii represents the scattered field using 100 sources in conventional MAS.. In fig. 3.7b. the difference in percentage between lines i and ii

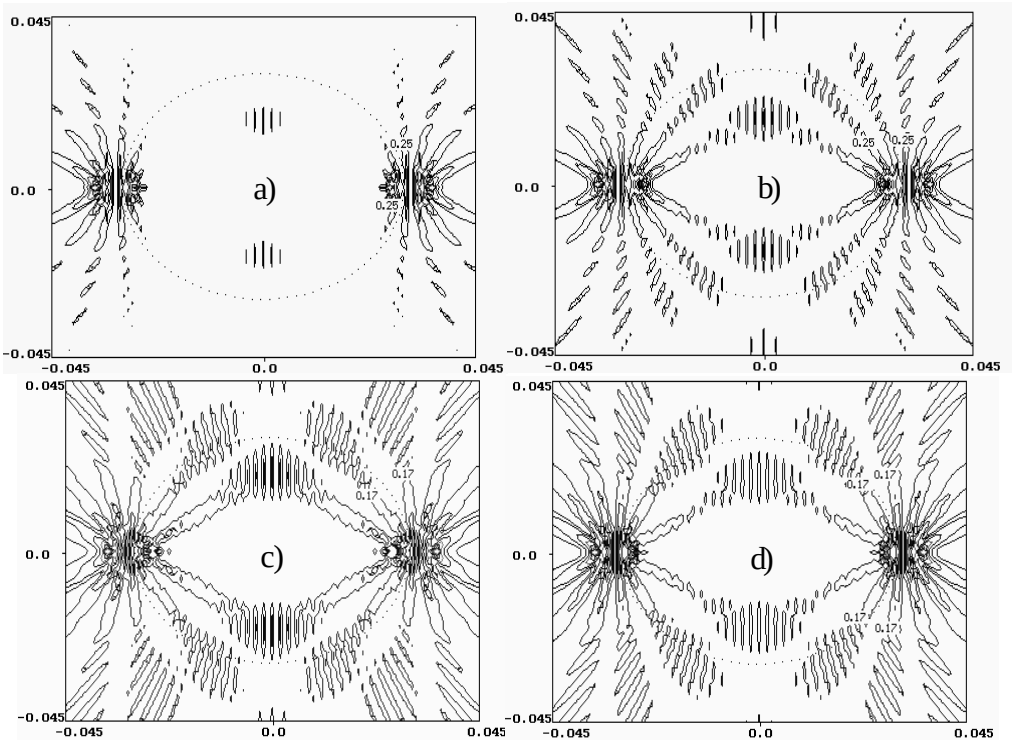

Figure 3.6: Scattered field by a) only two sources, b) four sources, c) eight sources and d) twelve sources for $ka = 64$

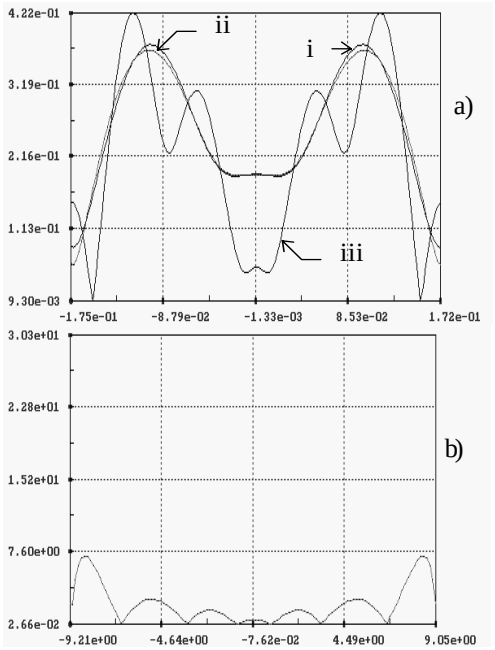

Figure 3.7: a) Field for a sector of 20 degrees at distance 0.039 by conventional MAS (line i 250 AS, line iii 150 AS) and by twelve sources placed at singularities (line ii), b) percentage difference between calculated field using conventional MAS with 250 AS and 12 sources placed in singularities positions

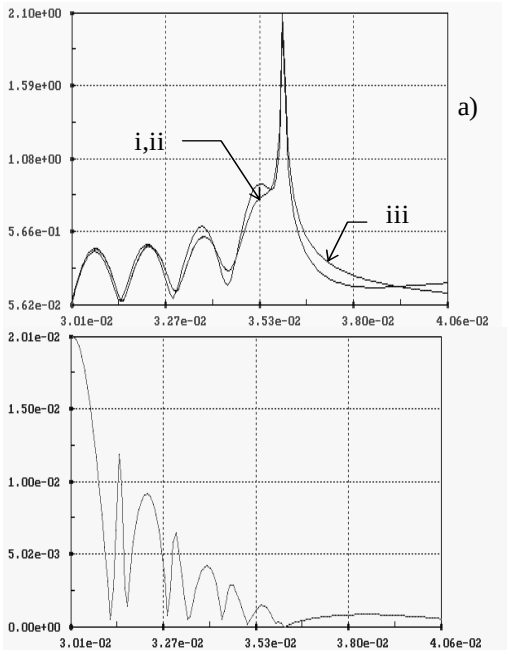

Figure 3.8: a) Field along x axis by conventional MAS (line i 250 AS, line iii 150 AS) and by twelve sources placed at singularities (line ii), b) absolute difference between calculated field using conventional MAS with 250 AS and 12 sources placed in singularities positions

is

presented. Note that the percentage difference even for high ka is very small with maximum less than 7.5%, and less than 3% in 10 degrees sector. Also in fig. 3.8a. the total field along x axis is presented for the three solutions, while in fig. 3.8(b). the absolute difference between lines i and ii is presented.

In this section the case of a large size cylindrical conductive scatterer is considered as shown in fig. 3.9, when an incident plane wave (linear source moved to infinity) is taken

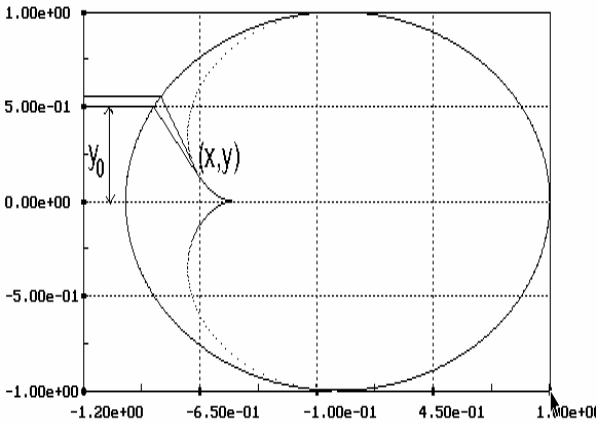

Figure 3.9: The caustic surface of a conductive cylinder illuminated by plane wave.

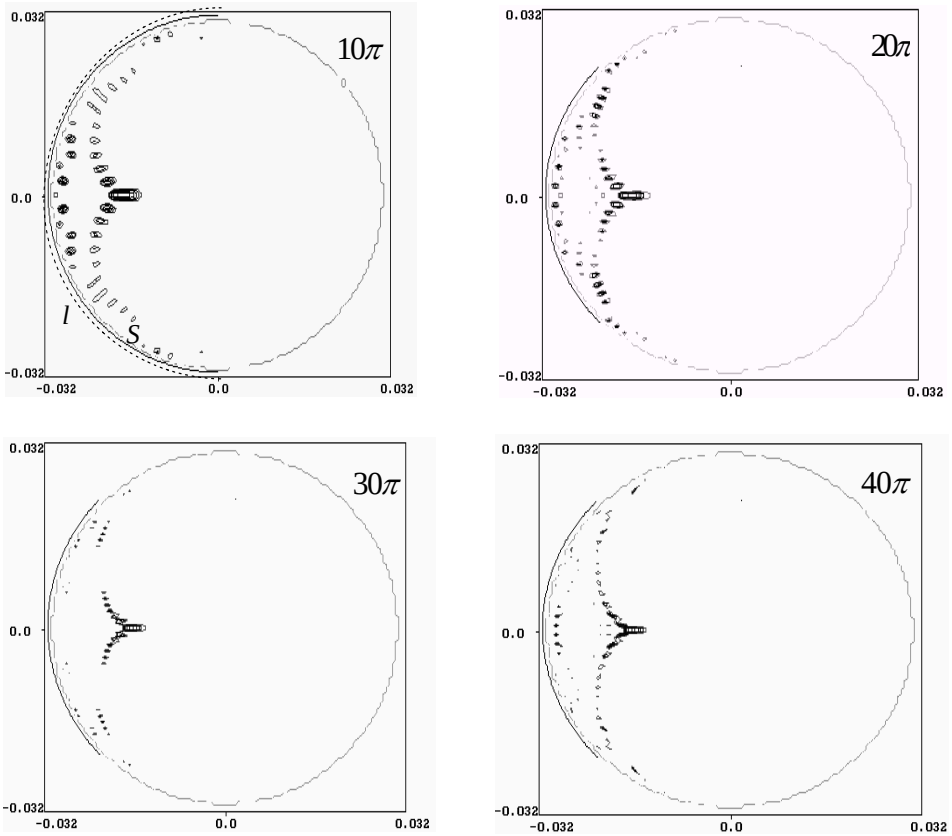

Figure 3.10: Scattered field singularities of perfectly conducted cylinder illuminated by a plane wave for a) ka = 40π **, b)** ka = 30π **, c)** ka = 20π **,** and **d)** ka = 10π

traveling along the *x* axis. It is known from the geometrical optics theory that the reflected rays from a beam of parallel lines as associated with a caustic contour described with the coordinates:

$$x = \left(\frac{1}{2} + \frac{y^2}{R^2}\right) \cdot \sqrt{R^2 - y^2} \quad (3.3)$$

$$y = y_0^3 \Big/ R^2 \quad (3.4)$$

where R is the cylinder radius and y_0 is the distance of the incident ray from the x-axis (see. fig. 3.9). The caustic contour is the focus of points associated with the zero order variation of two adjacent reflecting rays as shown also in fig. 3.9.

The investigation of the scattered field singularities for the problem of the perfectly contacted cylinder illuminated by a plane wave gave the following results:

1. It is obvious from fig. 3.10. that the scattered field singularities are distributed not continuously, but like bright illuminators located at distance of each other approximately half wavelength.

2. The scattered field singularities are distributed around the caustic surface (Scattered singularities for geometric optics). Caustic surface is the average, central surface for the scattered field singularities when wavelength tends to zero. (fig 3.10d).

3. The backscattered field is formed by central brightest area of the scattered field singularities, and for the problem of the cylinder, by two scattered field centers located along the normal line of the frontal surface with the distance of a half wavelength.

4. Scattering by Large Bodies

The previously mentioned distribution of Scattered Field Singularities inside a circular cylinder may be obtained also with some accuracy from the following consideration. First we will remind the concept of Fresnel's zones i.e. the parts of a surface where the phase change of incident field is equal to π. In the fig. 3.12 the Fresnel's zones are shown on a circular cylinder when it is illuminated by a point source (left picture) and a plane wave (right picture). The zones into which the cylinder is divided are formed by the wave front of the incident field and the distance between the neighboring borders of zones is $\lambda / 2$.

In the same manner we divide the scatterer surface (perfectly conducted cylinder) into Fresnel's zones. If now we continue the reflected filed from the first zone inside the scatterer it will be focused in one point (bright spot) as all waves continued from the first Fresnel's zone approach this spot with the phase delay not exceeding π. It means that all these waves give an effect of the field amplification in mentioned point. The waves continued from other zones give in average zero in the discussed point due to their different phase. The same is true for the second, third, etc., zones, but now the waves amplify each other in different points. Thus the set of points (bright spots) will be obtained. As the meter of fact the procedure of construction of this points is equivalent to the definition of caustics surface and thus the set of obtained points are actually the caustic points.

For each of the Fresnel's zones we now will choose the middle point on the surface of cylinder and find out the corresponding points on caustic surface. The set of caustic points given by this procedure, which is equivalent to the geometrical optics method is shown in fig. 3.13 (this picture is very similar to the distribution of bright points in the fig 3.11). By this the mentioned bright points will be obtained, but located on the caustic surface. As the matter of fact no surface of perfectly conducted cylinder is observed and the described points are those that one can actually see.

The above mentioned picture could be obtained using two different approaches and the second one comes from geometrical optics. Here must be also added that the picture very similar to one in fig. 3.12 can be given by integrating the physical optics currents for observation points inside the scatterer. As follows from described above the number of given bright spots or number of equations equals to the whole number of $N \approx 2ka / \pi + 1$. So the localization of Scattered Field Singularities can be found from scatterers' geometry and the

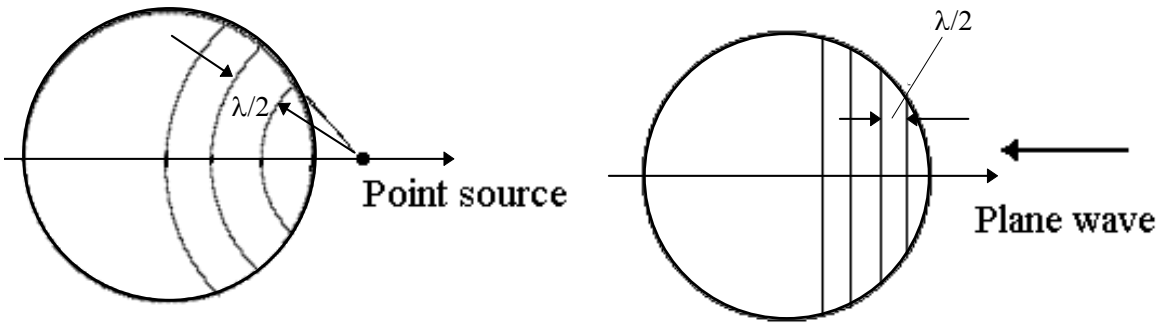

Figure 3.12: Fresnel's zones on the circular cylinder for incident fields of a point source and plane wave

type of incident field, i.e., dividing the whole scatterer into the Fresnel's zones and finding the corresponding points on caustic surface. It is important that this can be done before the solution of diffraction problem.

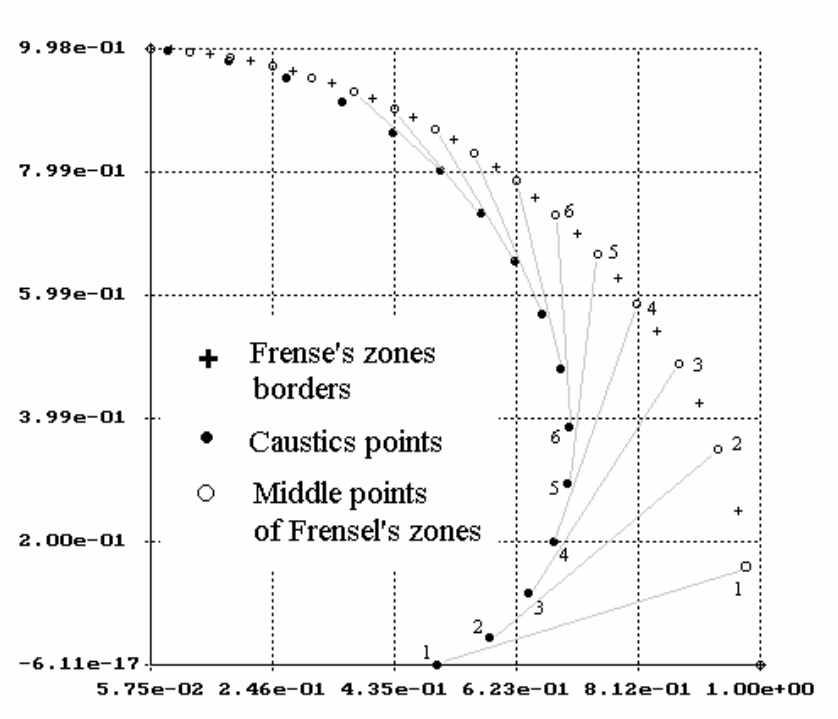

Figure 3.13: Caustics points corresponding to the centers of Fresnel's zones in case of plane wave incidence on the curricular cylinder. (upper right part of circle is shown)

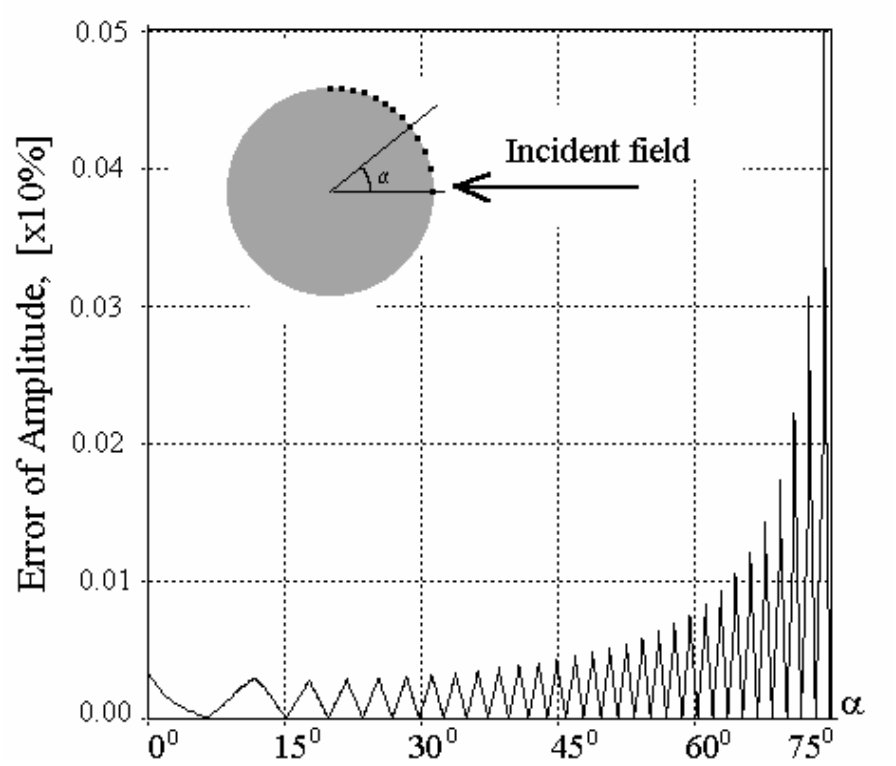

Figure 3.14: Amplitude of the total field along the cylinder surface (error of solution)

bright spots or number of equations equals to the whole number of $N \approx 2ka/\pi + 1$. So the localization of Scattered Field Singularities can be found from scatterers' geometry and the type of incident field, i.e., dividing the whole scatterer into the Fresnel's zones and finding the corresponding points on caustic surface. It is important that this can be done before the solution of diffraction problem.

Now inserting at each obtained point the sources which satisfy the boundary condition on the scatterer surface we will reconstruct the Scattered Field if assumption is made that each source radiates in the sector of correspondent zone. Of course the exact boundary condition is fulfilled in the middle point of each zone (where this was demanded), but the source in caustics point is the one that satisfies in average the boundary condition in the best way in comparison with other position of source. This comes from the meaning of the caustic point itself. Moreover it was noticed that the error in fulfillment of the boundary condition in the border of the zones is the same from two sources of neighboring zones. This is clearly seen in the fig 3.14: the boundary condition is exactly satisfied in the middle point of each zones (where it was demanded) and error increases in both direction from the middle point reaching its maximum value on the borders and again this value is the same for two neighboring zones.

Thus the whole field of all sources is continues in spite of there sector radiation. However, the exact distribution of the Scattered Field Singularities shown on fig 3.10 takes into account the creeping wave along the body's surface too.

One should note that in the mentioned case the phase difference of the incident field between two any neighboring points where the boundary condition is satisfied is 180^0 and between the corresponding sources on caustic surface - 90^0 i.e. α, $\alpha+90^0$, $\alpha+180^0$, etc. Therefor the sources form the running wave along the caustic surface.

In the all given examples and description the caustic points always where placed inside the scatterer. there are, however, such shapes of scatterers for which the caustics can appear outside the body. One of this case is the narrow elliptical cylinder illuminated by the plane wave. Angle of incidence is 30^o and $ka=100$. Semi-major and semi-minor axis of the ellipse are $a=1$ and $b=0.2$. The number of Auxiliary Sources, as well as the number of equations to

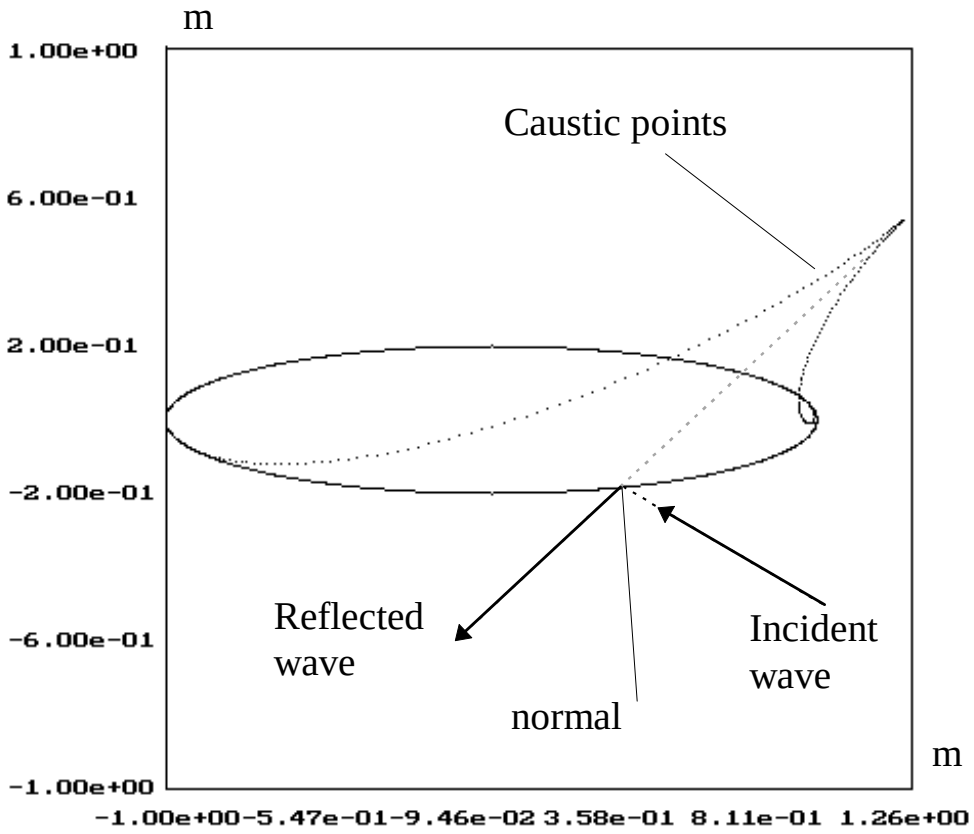

Figure 3.15: The set of caustics points corresponding to the problem shown in the figure 3.14

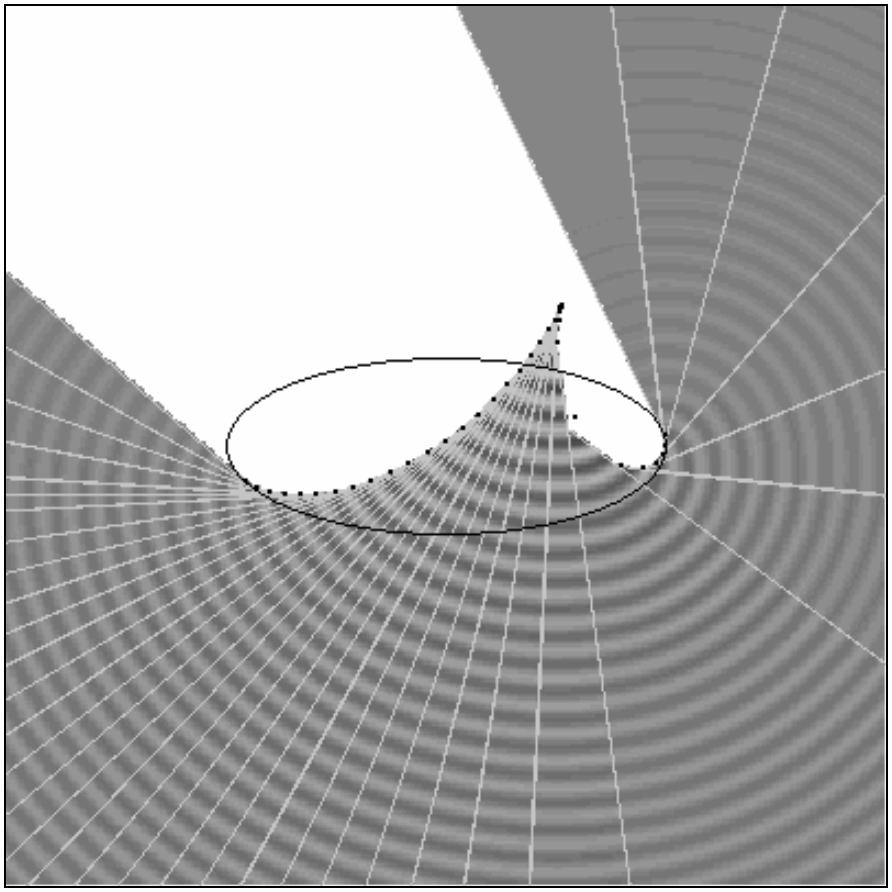

Figure 3.16: Real part of the scattered field in sectors corresponding to Fresnel's zones and to the Auxiliary Sources on caustic surface

solve is just 60.

The set of caustics points corresponding to the discussed problem is presented in the figure 3.15. This provides the accuracy of fulfillment of boundary condition within 1-3%. The precision of solution could be increased by further division of each Fresnel's zone into two or more parts. The scattered field in illuminated area is presented in fig. 3.16. The corresponding sectors are shown to demonstrate how the solution is constructed.

As concerns to the shadow zone, the field in it was calculated by the set of Auxiliary Sources placed in the illuminated side of the scatterer and tiding up their field with the incident field at the back side. The scattered field is shown in the fig 3.16. The wave number could be easily increased, but it was limited with ka=100 to avoid the problem with picture resolution in this paper.

Thus the knowledge of Scattered Field Singularities localization allows to reduce sharply the necessary computer resources and investigate the diffraction problems for almost optical waves. This method should be efficient for convex scatterers. If the scatterer is concave the possible secondary, third, etc., reflections should be taken into account. The same is true when there is system of two and more scatterers.

In case of dielectric bodies along with the caustic for reflected rays the caustic for refracted rays should be taken into account to reconstruct the field inside the scatterer.

In the end we must note that the presented algorithm is very close to the geometrical optics implementation and thus the accuracy is high for large compared to wavelength bodies. The main advantage of described technique is that the best location for Auxiliary Sources is found which allows to represent the scattered field in corresponding sector only by one source, solving just one algebraic equation. As the number of such sectors equals to the number of Fresnel's zones on scatterer surface the total number of unknown is of order $N \approx 2ka/\pi + 1$ that provides accuracy of several percents.

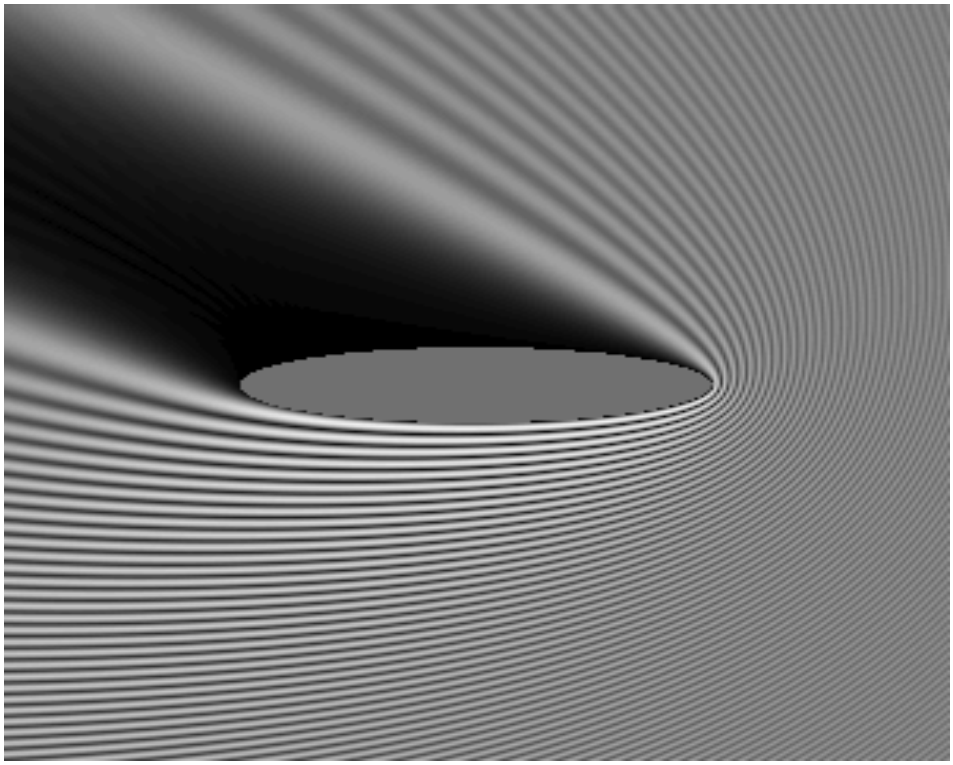

Figure 3.16: The absolute value of the total field. (incident plus scattered)

IV. The Inverse Problem Solution

1. The General Algorithm of the Near Field Reconstruction

There are many publications concerning the various types and methods of solution of inverse electrodynamics and antenna synthesis problems. The general formulation of antenna synthesis problem by the pattern has itself various approaches. There are also many approaches for optimization of the antenna shape and elements placement [44].

It is known that the inverse problems do not have the unique solution. For example, for a specific pattern in an antenna design problem, different current distributions on the different surfaces can be introduced. The main problem is to obtain such distribution of currents that produces the minimum of reactive field in near zone so that the whole feeding energy is transmitted into the traveling wave. Such antenna is referred as “well matched antenna”.

It is assumed that any diagram should have its own unique singularities. On the other hands it is known that a traveling wave is analytical everywhere except the area of its excitation. This is the area of singularities of radiated field which form this traveling wave and therefore its diagram.

The problem to be solved is the design of a “well matched antenna” that will produce a given far field pattern. This is equivalent to the determination of the singularities of the specific pattern. Thus the near field has to be determined as shown previously.

For this purpose an auxiliary circular antenna is introduced [38]. The far field of this antenna is calculated and it is matched with the given far field pattern by distributing the auxiliary sources on the auxiliary surface inside the auxiliary antenna. It is obvious that the near field of this auxiliary sources can be easily calculated, therefor using the method of visualization of scattered field singularities described before the singularities of the given pattern (e.g. the location of the antenna dipoles) is determined.

In detail consider the 2D case, where an antenna with a pattern $F(\varphi)$ has to be designed. First of all it is necessary to obtain the near field corresponding to the specified diagram $F(\varphi)$. This could be done by distributing N sources of $H_0^{(1)}(kr)$ type on some curve S covering an area D. In this case the S is chosen to be the circle of diameter d. Here should be noted that diameter d must not be less than some definite value to provide the necessary width of the main lobe. This condition is $d > \lambda/\Theta$, where λ is the wavelength and Θ is the width of the main lobe. The field radiated by these sources will be:

$$E(r) = \sum_{n=0}^{N} a_n H_0^{(1)}(k(r - r_n)) \quad (4.1)$$

While the far field pattern will be determined by the asymptotic approach of the expression (4.1), using the fact that $\lim_{r\to\infty} H_0^{(1)}(kr) = \sqrt{\frac{2}{\pi kr}} e^{-ikr + i\pi/4}$. So (4.1) becomes:

$$\lim_{r\to\infty} E(r) = \sqrt{\frac{2}{\pi kr}} \sum_{n=0}^{N} a_n e^{-ik(x_n \cos(\varphi) + y_n \sin(\varphi)) + i\frac{\pi}{4}} \quad (4.2)$$

Using the collocation method to bind the radiated field of these sources in M directions with the given one in far zone the system of liner equations will be obtained

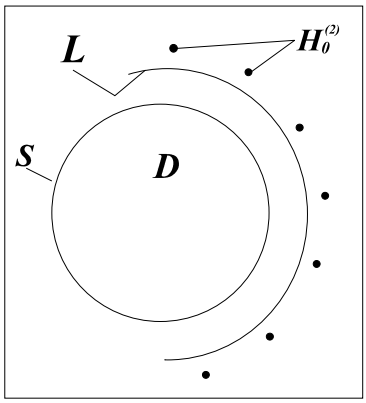

Figure 4.1: The geometry of the near field reconstructing algorithm.

$$\sum_{n=0}^{N} a_n e^{-ik(x_n \cos\varphi_m - y_n \sin\varphi_m)} = F(\varphi_m) \quad M = 1,2,\ldots,m\,. \quad (4.3)$$

Solving the system of liner equations (4.3) the coefficients a_n can be determined. These a_n are the complex amplitudes of the sources that give the desired diagram. The precision of this solution depends on the number *N* of collocation points. So after achieving the diagram with the desirable accuracy the field of such sources is known everywhere outside the area *D* including the near field (4.1). It must be noted that the reactive field of these sources decreases as the diameter *d* increases, since no standing wave is described by these sources, area *D* should be taken big enough to provide low reactive part of the field in near zone.

As the near field is known outside the area *D* the second step is to continue it analytically inside *D* using the following scheme. Taking into account all mentioned above the extension of the near field also will be unique up to the singularities regarding the chosen area *D*. Let us choose some curve *L* outside *D*, where the near field is known. Assume that *N* sources $H_0^{(2)}(kr)$ are placed at some distance from the curve *L*. These sources acts as absorbers of the wave, traveling from the area *D* to infinity. The *N* chosen sources will reconstruct the field on the curve *L* if

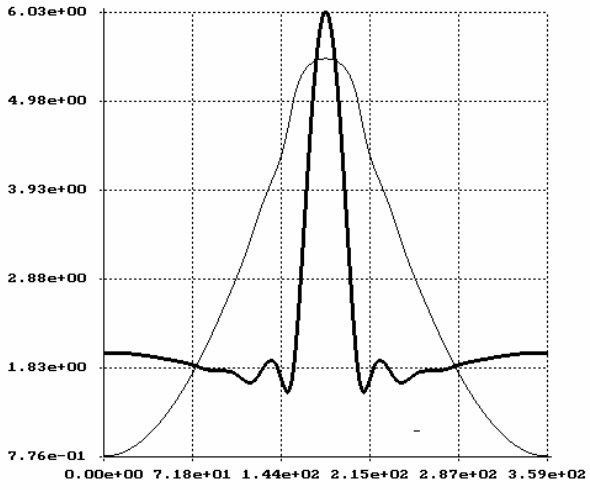

Fig. 4.2: Phase and amplitude diagram

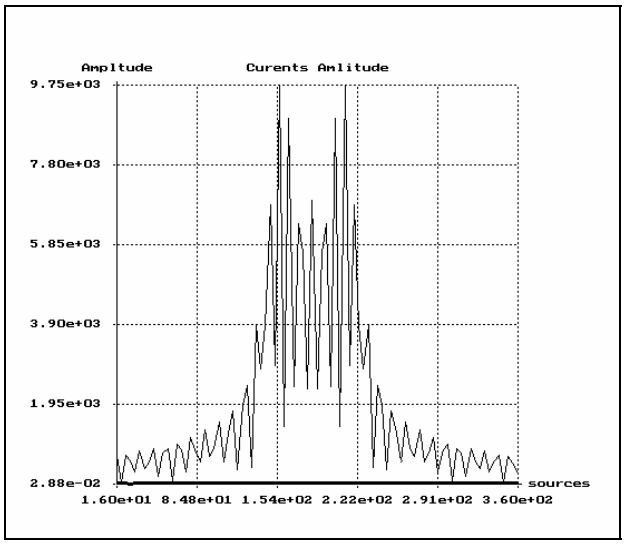

Figure 4.3:

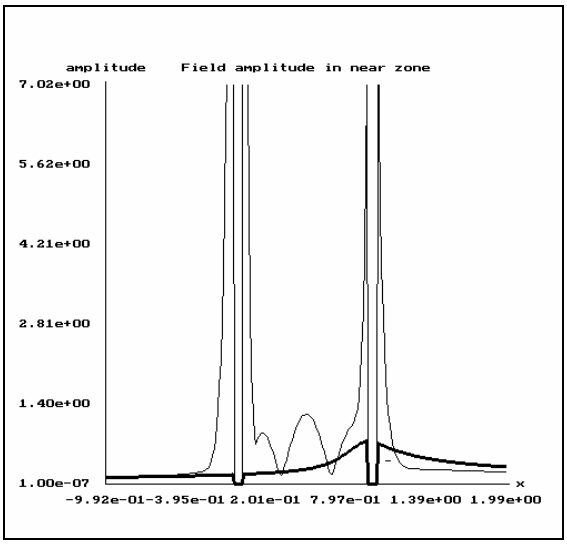

Figure 4.4:

$$\sum_{n=1}^{N} b_n H_0^{(2)}\left(k\left(r_n - r_m\right)\right) = E\left(r_m\right), \quad (4.4)$$

where b_n - is the complex amplitude of n source and $E(r_m)$ is the near field value in corresponding point on the curve L. If the number N is big enough, the reconstructed field tends to the real one. Since there is a matching of fields on the curve L there must be also matching inside the area D up to the area of singularities of the given near field. So the numerical analytical continuation of the near field will be found inside area D.

Further it could be shown that the appropriate phase distribution in far zone can significantly decrease the reactive part of near field. In other words the radiated system becomes well matched and all feeding energy is transformed into the traveling wave.

2. Solution of Some Problems

a) Consider as an example the far field amplitude and phase pattern of the field scattered by the perfectly conductive cylinder illuminated by the plane wave shown in fig. 4.2. Suppose also there are the same far field amplitude but with constant phase diagram. For these two cases the described above algorithm was applied and in fig. 4.3 the amplitudes of the auxiliary sources of circular auxiliary antenna are presented: the light line for constant far field phase diagram and the bold line for far field phase diagram of the scattered by the Perfect Conductor cylinder field. The amplitudes for the case with constant phase are of order 10^3 while for the second case are of order 10^{-2}.

Additionally fig. 4.4 shows the electric field distribution along the axis y=0 for both cases. This figure also shows how the reactive field in near zone is increased if the phase information in far zone is lost or do not considered.

b) Let us consider one more example for optimizing the inverse problem solution. The aim is to synthesise a given directivity diagram, originally generated by two EM wave sources, placing at some distance of several wavelength from each other. The corresponding patern is

shown in fig.4.5 and the near field in fig. 4.6. With the sources placing on the curcle it is possible to reconstruct this directivity diagram as was discribed above (see formula 4.1 and 4.4). The result is shown in fig. 4.7. Then using the set of absorbing sources the near field is continued inside the circle. The field obtained in such way gives two sharp maximums near the area where the original sources was placed (fig 4.8). Therefor the information about field singularities is embaded, which are actually in the points of original sources, and one can note that this information was given only by consideration the directivity diagram without previous knowledge of original sources. It is now obvious that placing in this area two sources the disired radiation pattern in the most optimal way can be obtained.

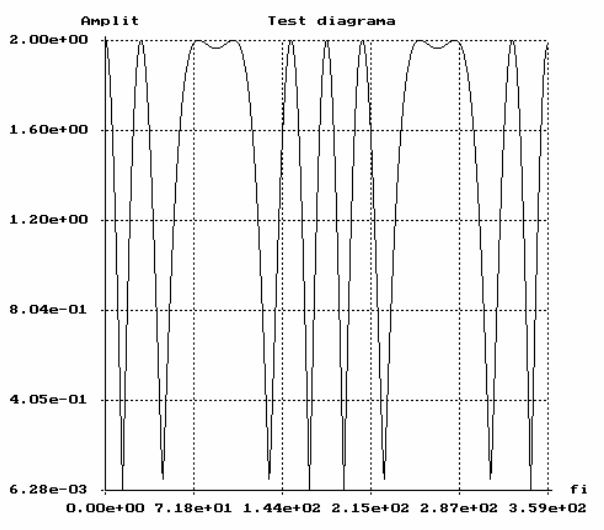

Figure 4.5: Radiation pattern requested

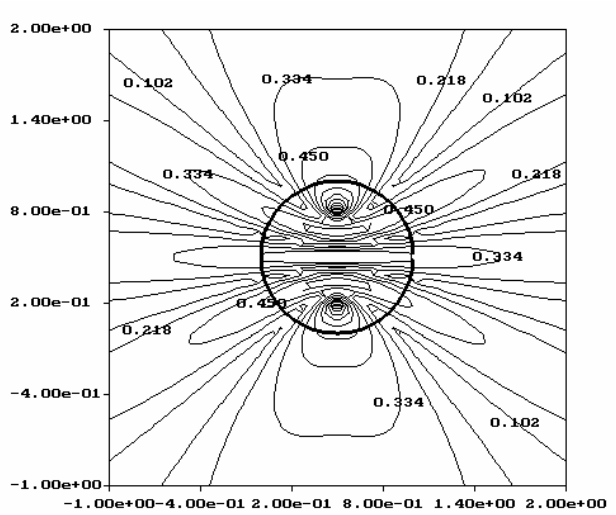

Figure 4.6: Field corresponding to the radiation pattern

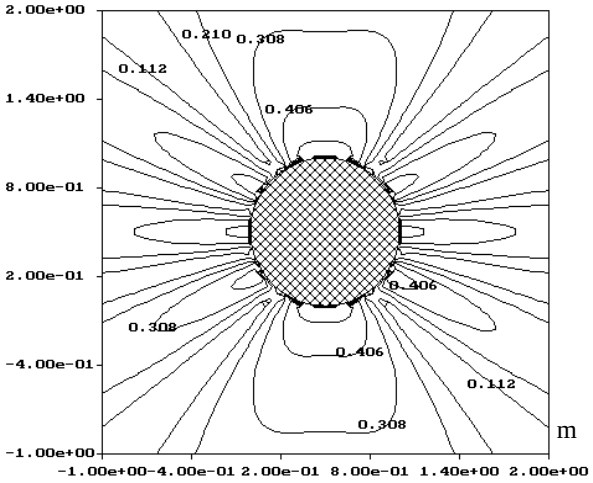

Figure 4.7: Reconstructed field.

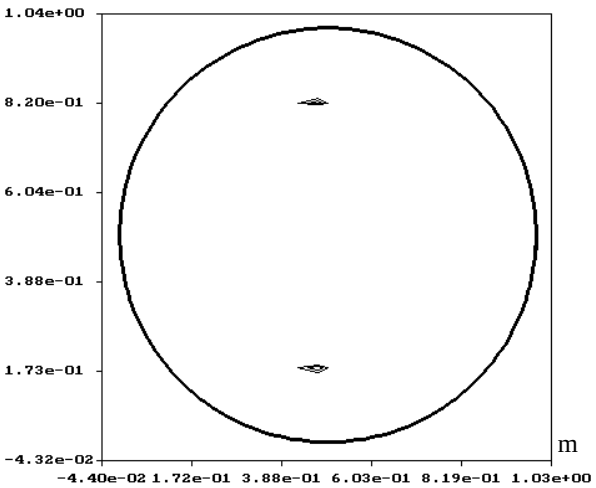

Figure 4.8: Reconstructed coordinates of the sources to be found.

V. The Method of Auxiliary Sources for Scattering Problems in Time Domain

1. Formulation of the problem

The Method of Auxiliary Sources (Method of Auxiliary Sources) has been extensively applied to the wide class of electromagnetic problems. The extension of Method of Auxiliary Sources into time domain is presented in this chapter. It provides a fast algorithm for simulation and visualization of electromagnetic periodical and transient processes in time domain [39,40]. The transient scattering on the cylinder with longitudinal slot is considered as an example.

Consider the scattering problem of a conductive scatterer of surface S illuminated by an incident field $\vec{\mathrm{E}}^{\mathrm{inc}} = (\vec{\mathrm{r}}, \mathrm{t})$, $\vec{\mathrm{H}}^{\mathrm{inc}} = (\vec{\mathrm{r}}, \mathrm{t})$. The unknown scattered field should satisfy the wave equation:

$$\nabla^2 \vec{E}^{sc}(\vec{r},t) - \frac{1}{c^2}\frac{\partial^2 \vec{E}^{sc}(\vec{r},t)}{\partial t^2} = 0 \quad \vec{r} \in \overline{D} \quad (5.1)$$

and the boundary conditions, as

$$\hat{\mathrm{W}}\left\{\vec{\mathrm{E}}^{\mathrm{sc}}(\vec{\mathrm{r}},\mathrm{t}) - \vec{\mathrm{E}}^{\mathrm{inc}}(\vec{\mathrm{r}},\mathrm{t})\right\} = 0 \quad \vec{\mathrm{r}} \in \mathrm{S}. \quad (5.2)$$

According to the Method of Auxiliary Sources we will find the solution of this problem expressed by the fundamental solution of the equation (4.1). Again in this case this fundamental solution are presented by some Auxiliary Sources distributed on the shifted inside the scatterer contour S_0.

Location and the type of the auxiliary sources are determined by the incident field and by the main singularities of the scattered fields. If these singularities are taken into account and

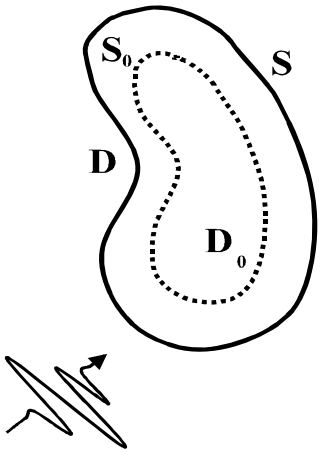

Figure 5.1: Geometry of the problem.

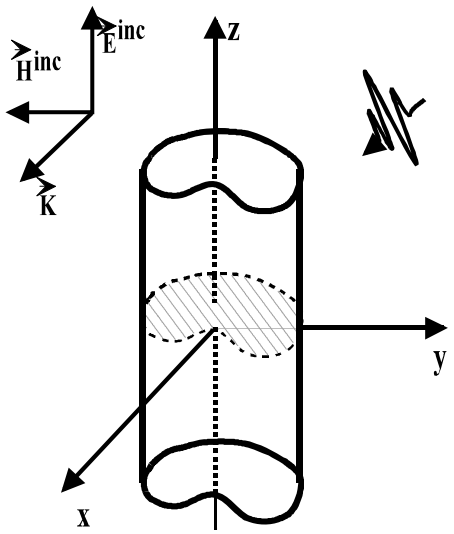

Figure 5.2: Geometry of 2D Scattering problem. E-Polarization

the auxiliary parameters are chosen correctly, the method becomes significant efficient.

2. 2D case, E-polarization

Let us choose some auxiliary contour and points $\left\{x_n^{S_0}, y_n^{S_0}\right\}_{n=1}^{N}$ on it. On the main contour **S** the points of collocations $\left\{x_k^{S}, y_k^{S}\right\}_{k=1}^{N}$ are distributed.

The numbering of points is taken in a such a way that the distance between points with the same numbers on **S** and on $\mathbf{S_o}$ is minimal. One additional restriction that arises from time domain methods is:

$R_{n,n\pm1} \geq c\Delta t$

where $R_{k,n} = \sqrt{\left(x_k^S - x_n^{S_0}\right)^2 + \left(y_k^S - y_n^{S_0}\right)^2}$

The two-dimensional Green functions corresponding to the given geometry is used as the basis functions in this problem:

$$E_N^{sc}(x,y,t) = \sum_{n=1}^{N} E_n^{aux}(x,y,t) \quad (5.3)$$

$$E_n^{aux}(x,y,t) = \frac{1}{2\pi} \int_0^{t-R_0/c} \frac{f_n(\tau)\, d\tau}{\sqrt{(t-\tau)^2 - \left(\frac{R_n}{c}\right)^2}} \quad (5.4)$$

where f_n- is unknown "magnitude" of the n-th auxiliary source and $R_n = \sqrt{\left(x - x_n^{S_0}\right)^2 + \left(y - y_n^{S_0}\right)^2}$. The field (5.3) must satisfy the boundary condition

$$\left(E^{inc} + \sum_{n=1}^{N} E_n^{aux} \right)\Bigg|_S = 0 \quad (5.5)$$

The sum in (5.5) can be broken into two parts to perform integration numerically at the upper limit.

$$E^{inc}(x_k,y_k,t) + \frac{1}{2\pi} \sum_{\substack{1 \\ n\neq k}}^{N} \int_0^{t-r_{nk}/c} \frac{f_n(\tau)d\tau}{\sqrt{(t-\tau)^2 - (r_{nk}/c)^2}} + \frac{1}{2\pi} \int_0^{t-r_{kk}/c} \frac{f_k(\tau)d\tau}{\sqrt{(t-\tau)^2 - (r_{kk}/c)^2}} = 0 \quad (5.6)$$

The first sum represents the contribution of all auxiliary sources except of the *k*-th and the second is the contribution of the *k*-th source. The function $f_n(\tau)$ is known for all moments except for $t\text{-}r_{kk}/c$. The integration in (5.6) is performed analytically at each step of time under assumption that the function $f_n(\tau)$ changes linearly at every step up to the time moment $(M\text{-}1)*\Delta t$, where *M* is such that $0 < t - r_{nk}/c - M\cdot\Delta t < \Delta t$. That is, each integral in (5.6) is presented as:

$$\int_0^{t-r_{nk}/c} = \int_0^{(M-1)\Delta t} + \int_{(M-1)\Delta t}^{t-r_{nk}/c} \quad (5.7)$$

The second term in (5.7) is evaluated analytically. For this purpose the function $f_n(\tau)$ is approximated by three-point interpolation formula.

The $f_k(t)$ must be evaluated for the moment $t-r_{kk}/c$ at this step of algorithm. This evaluation can be done analytically. For this purpose the function $f_k(t)$ is approximated by the three-point interpolation formula, based on the earlier times and the time $t-r_{kk}/c$, where $f_k(t)$ is unknown. This unknown value is implicitly presented in approximation coefficients, that make it possible to calculate it from (5.6).

At the every step of procedure all of the N sources must be determined before the next step will be proceeded. In such approach one important condition must be satisfied:

$$r_{kk} - r_{nk} < c\Delta t \quad (5.8)$$

where $k,n=1..N$, $k \neq n$. This condition guarantees that at every step all necessary $f_n(\tau)$ are already known from previous steps.

Therefor it is possible to solve the equation (5.6) reducing it to a recurrence formula in time domain for $f_n(\tau)$ function and perform the calculation simply marching on in time.

After determination of all functions $f_n(\tau)$ for all necessary moments it is possible to calculate the scattered field at any point outside the contour L as follows:

$$E(x,y,t) = \frac{1}{2\pi}\sum_{n=1}^{N}\int_0^{t-R/c}\frac{f_n(\tau)d\tau}{\sqrt{(t-\tau)^2-(R/c)^2}} \quad (5.9)$$

where R is the distance between the observation point and n-th auxiliary source.

Moreover it is possible to calculate the field directly on the contour **S**, that allows to check the validation of the solution. The total field on the contour **S** must satisfy condition (5.5). Of course at the point of collocation this condition is satisfied exactly, but estimation of the field in other points of the contour **S**, serves as a criterion for the validation of the solution. Particularly, this estimation could be done as follows:

$$\sigma = \sqrt{\frac{\int_S dl\int_0^t (E^{inc}+E^{sc})^2\,dt}{\int_S dl\int_0^t (E^{inc})^2\,dt}}\cdot 100\% \quad (5.10)$$

The selection of the auxiliary contour $\mathbf{S_o}$ is one of the important question in the Method of Auxiliary Sources. This contour, of course, depends on the geometry of scatterer. Usually $\mathbf{S_o}$ is chosen to be similar to the cross-section contour **S** in such way that auxiliary sources are located inside the scatterer at some distance from the **S**. This distance is also depending on the number of sources *N*. As *N* increases, the distance is getting shorter. But it must be noted that the number *N* can be selected several times less than the number of surface segmentation needed for the surface integral methods for the same precision of solution. Particularly this advantage appears for the solid scatterers.

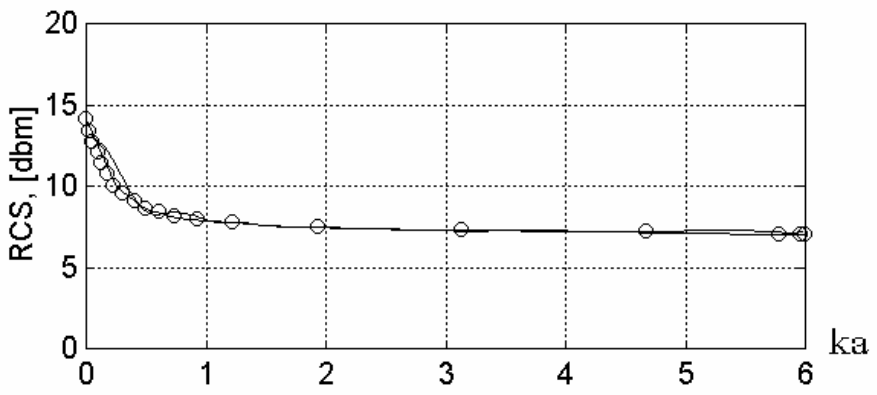

Figure 5.3: Back scattering Radar Cross Section (RCS); o - Exact frequency domain solution, — - FFT of time domain solution

3. Numerical results

The algorithm has been tested for various shapes and incident pulses. Some of the results are shown below for a plane incident Gaussian pulse.

$$E^{inc} = (\alpha / \sqrt{\pi}) \exp(-\alpha^2 (ct - x)^2) \quad (5.11)$$

with the $\alpha = 2 \ \ m^{-1}$. The length of the pulse in this case is approximately $ct = 2.6$ m.

The circular cylinder was chosen as a model structure to compare results with the well known analytical solution for this problem. Another scatterers were ellipsoidal cylinder, the thin strip and the circular cylinder with the longitudinal slot. The solution is in a good agreement with the results given by MoM in time domain. Fig. 5.3 illustrates the backscattering cross section, that is given by implying the FFT to the backscattering field. It is seen the good agreement with frequency-domain solution. The fulfillment of the boundary conditions calculated by the formula (15) gives $\sigma = 3\%$ for *N*=32 and 1.4% for *N*=64.

Transient auxiliary currents are shown for ellipsoidal cylinder with semiaxis *a/b*=0.4 on the Fig.5.4.

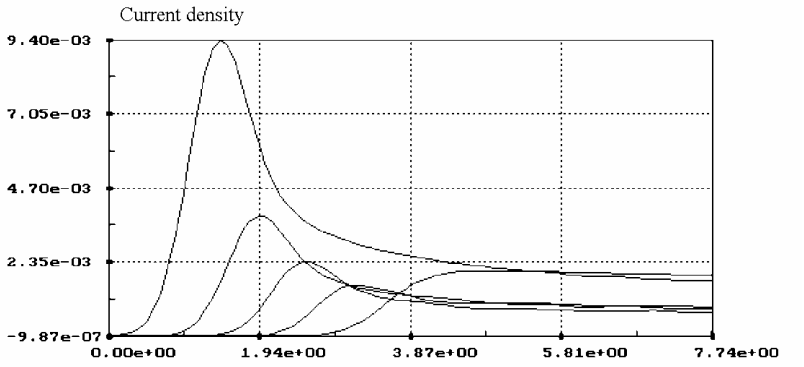

Figure 5.4: Transient auxiliary currents for ellipsoidal cylinder (N=32) at five equidistant points

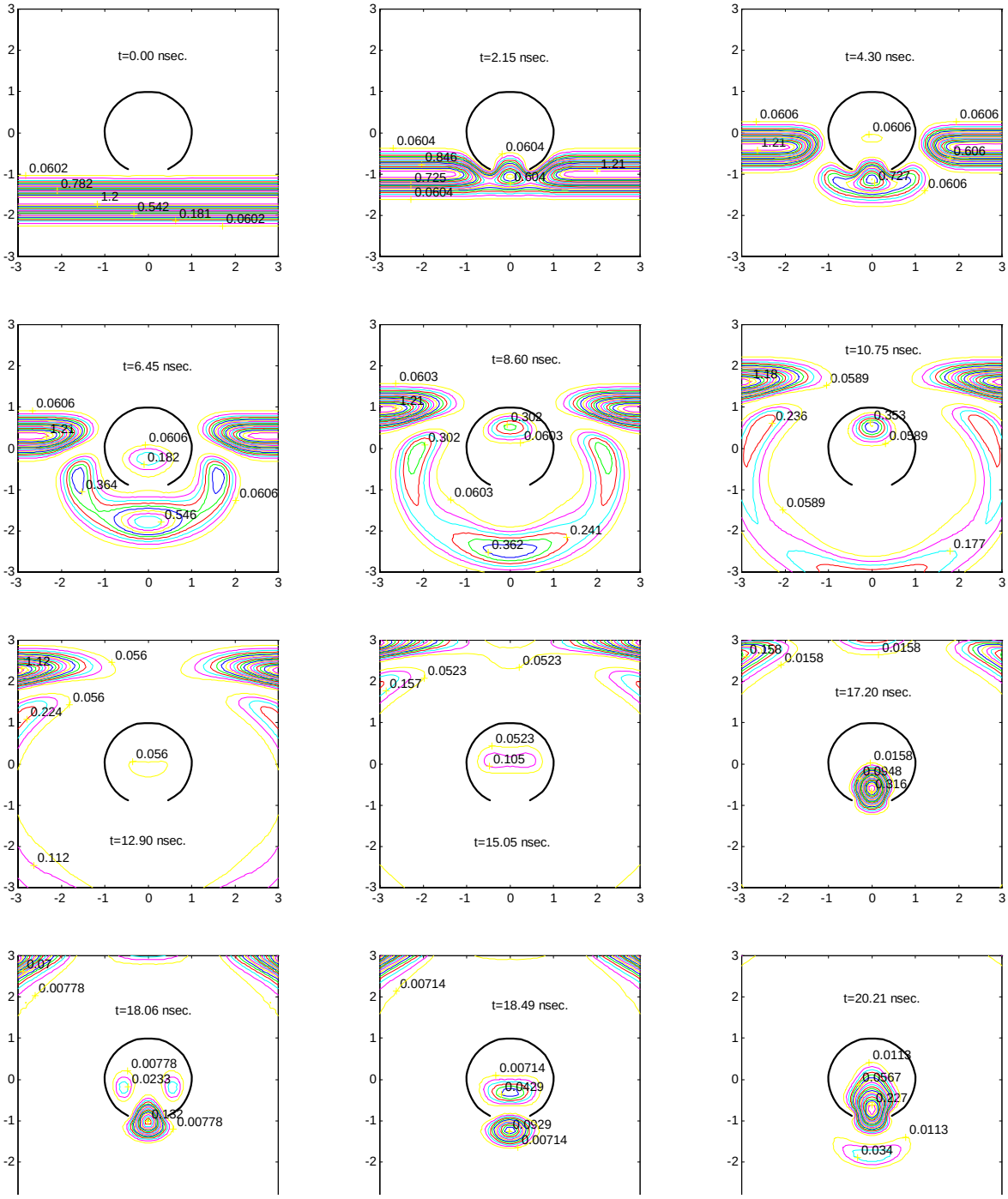
t=0.00 nsec.
0.0602
0.782
1.2
0.542
0.181
0.0602
t=2.15 nsec.
0.0604
0.846
0.0604
0.725
0.0604
0.604
1.21
t=4.30 nsec.
0.0606
0.0606
0.0606
1.21
0.606
0.727
0.0606
t=6.45 nsec.
0.0606
1.21
0.0606
0.182
0.364
0.0606
0.546
t=8.60 nsec.
0.0603
1.21
0.302
0.302
0.0603
0.0603
0.241
0.362
t=10.75 nsec.
1.18
0.0589
0.236
0.353
0.0589
0.0589
0.177
1.12
0.056
0.056
0.224
0.056
t=12.90 nsec.
0.112
0.0523
0.0523
0.157
0.0523
0.105
t=15.05 nsec.
0.158
0.0158
0.0158
t=17.20 nsec.
0.0158
0.0948
0.316
0.07
0.00778
t=18.06 nsec.
0.00778
0.0233
0.132
0.00778
0.00714
t=18.49 nsec.
0.00714
0.0429
0.0929
0.00714
t=20.21 nsec.
0.0113
0.0567
0.227
0.0113
0.034

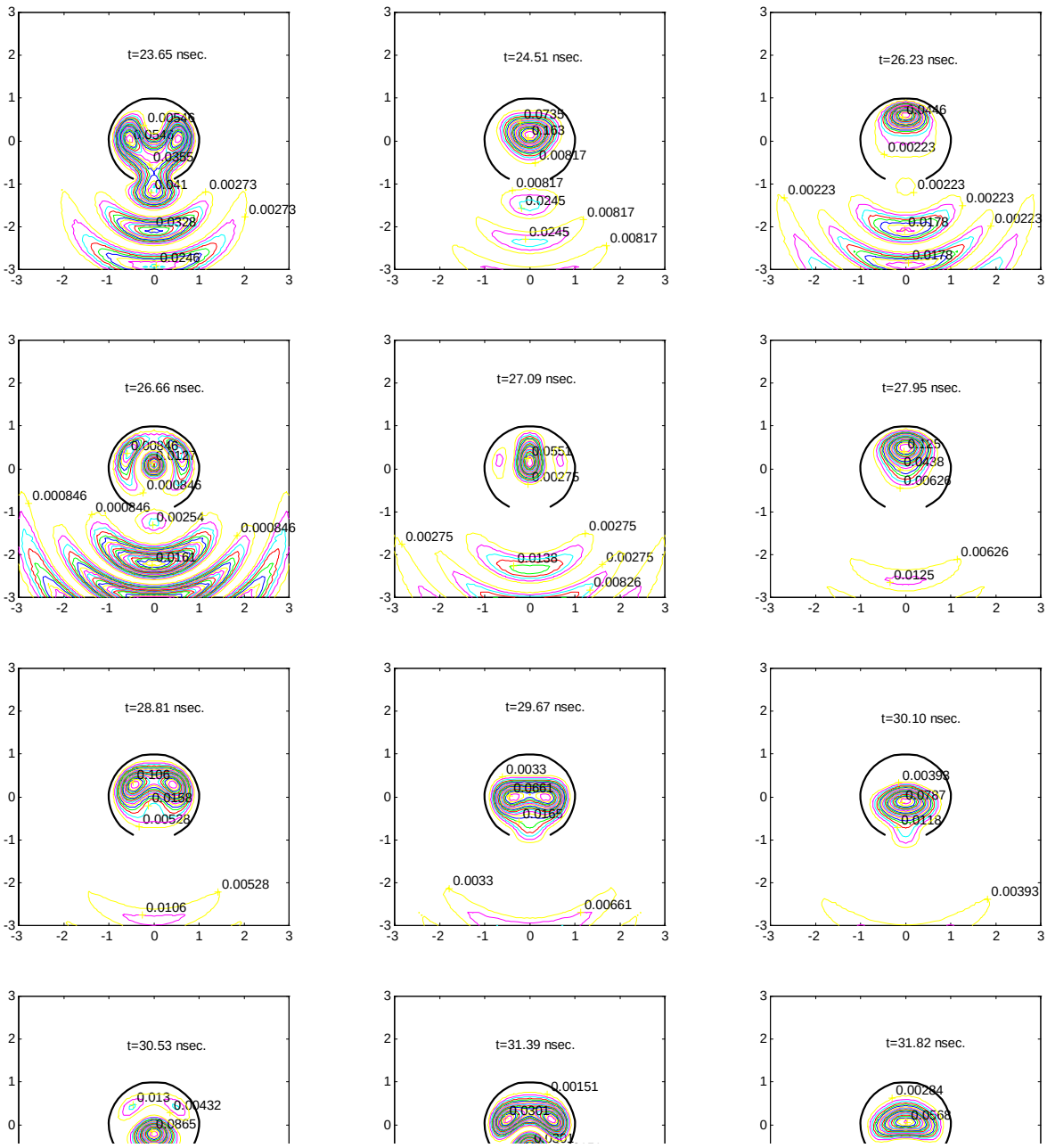

Figure 5.5: Near field of the circular cylinder with longitudinal slot at the different time moments.

Finally the transient scattering on a circular cylinder with longitudinal slot is demonstrated. Figure 5.5 demonstrates the near field at different time moments.

It is clearly seen how the incident field penetrates inside the cylinder through the slot aperture. At the late time, when the incident pulse is gone, one can note how the eigenfield of the inner area is created step by step and energy is radiated out of the cylinder through the slot. As the incident pulse is Gaussian, the dominant eigenfields are of the first resonance frequencies.

The testing of the Auxiliary Sources Method in Time Domain for different two-dimensional scattering problems demonstrates that it is much effective in comparison to surface integral methods as in a time as well as in a frequency domain. In all tested problems the same precision of solution was achieved using the number of auxiliary sources several times less than number of surface segmentation in integral methods. Particularly this advantage is seen for closed contour **S**, when it is possible to place the auxiliary sources inside the body. The typical time, which is needed to find out the magnitudes of all auxiliary sources on a Pentium-90 MHz based computer varies from 5 sec to 60 sec. depending on the number N of these sources. For instance the problem for circular cylinder took just 10 sec for determination of all necessary sources. The same time is needed solving the problem with open contour **S** of the cylinder (for example with longitudinal slot).

In conclusion the above technique can be considered as a fast tool for solving different transient scattering problems, which have a large number of applications in technology.

Conclusion

In the beginning of this book the brief description of the Method of Auxiliary Sources, suggested by Kupradze, is given. The Method of Auxiliary Sources was intensively used during the last 3 decades as one of the most powerful tools for numerical solution of mathematical physic problems.

This method was successfully implemented by many researchers in a wide group of areas such as electromagnetism, theory of elasticity and geophysics, electrostatic problems, hydrodynamics and diffraction of acoustic waves [15,18-22,46]. Despite the high efficiency of the method, it has been observed that in some cases the numerical implementation of the method shows poor convergence or rarely even divergence of solution. These problems were discussed in [18,20,21,30,31]. Basically these problems are connected to the well known "Rayleigh hypothesis". In this book an attempt was made to clarify these problems.

During the implementation of the method it became obvious that significant difficulties arises if the physical properties of scattered fields like Scattered Fields Singularities and resonance of the auxiliary surfaces are not concerned. On the other hand if the implementers do consider these physical properties the efficiency of the method is sharply increased since both accuracy and computational resources are optimized.

Based on the physical meaning and the main peculiarities of the Scattered Fields Singularities efficient utilization of the Method of Auxiliary Sources in applied electrodynamics is shown. Besides, in order to optimize the method, the high theoretical interesting issue of the localization of the Scattered Fields Singularities as well as their behavior for various frequencies and different shape of scatterer and finally how they turn into caustics for optics when wave-length goes to zero is studied.

Furthermore, a new approach that leads to the highly interesting source visualization technique based on the Method of Auxiliary Sources is proposed. This approach, firstly used in this book, has been used for the visualization of the Scattered Field Singularities, but it is obvious that it also expands the appliance of the Method of Auxiliary Sources to a variety of other electromagnetic problems.

To this end, the directions were given in order to expand the usage of the Method of Auxiliary Sources for large body scattering problems. The innovation is the introduction of the Scattered Field Singularities as the areas where the auxiliary sources should be placed in order to minimize the computational cost. Some examples are considered and the improvises of the method using the knowledge of Scattered Field Singularities are shown. In suggested Scattered Field Singularities visualization method 'absorbers' (e.g. functions describing field pointing them) are used. The latter method is used for the localization of the Scattered Field Singularities for the cylinder and the behavior of these singularities while wavelength changes is also shown.

Finally, the extension of the Method of Auxiliary Sources into time domain is presented. The implementation of the method provides a fast algorithm for simulation and visualization of transient electromagnetic processes in time domain.

References

[1] Kupradze V. Dynamical Problems in Elasticity, Progress in Solid Mechanics 3. Amsterdam, 1963.

[2] Kupradze V. About approximates solution of mathematical physics problem. Success of Mathematical Sciences, Moscow.22. N2 1967, 59-107.

[3] Vekua I.N. About a metaharmonic functions - Proceedings of Tbilisi Mathemat. institute, Acad. of Science, Georgia, 12 (1943), 105-174.

[4] Vekua I.N. Reports of Academy of Science of USSR, 1953 v.90, N5, p.715.

[5] Vekua I.N. New Methods for Solving Elliptic Equations, translated form Russian by D.E. Brown, 1967. pp. 84-88 John Wiley, New York.

[6] Millar R.F. Proc. Cambr. Phil. Soc. 1969, v.65, p.773.

[7] Millar R.F. Electron. Letters 1969. v.5 p.416.

[8] Millar R.F. Radio Science. 1973 v.8. N8.9 pp.785-796.

[9] Yasuura K. (1961) J. Inst. Elec. Communun. Eng. Jap. 44(6), 901-909.

[10] Yasuura K. Ikuno H. 1971. On the modified Reylaigh hypothesis and MMM Inter. Symp. on Anten. and Propag. Sendai Japan pp.173-174.

[11] Okuno Y. (1994) A duality Relationship between Scattering Field and current density calculation in the Yasuura Method.MMET, URSI, Kharkov, Ukraine pp.278-281

[12] Waterman P.C. (1969) New formulation of acoustic scattering J.Acoust. Soc. Amer, 417-29.

[13] Waterman P.C. (1971) Symmetry, unitarity and geometry in EM scattering, Phys.Rev.Sect D, Ser 3 3(4), 825-839.

[14] Mittra R., Wilton K. 1969. Proc.IEEE, 57(11), 2064-2065.

[15] Eremin Yu.A. Lebedev O.A. Sveshnikov A.G. 1988. Radioeng. and Electr. Acad. of Scie USSR. Nauka, v.33, N10, 2076-2083.

[16] Eremin Yu.A. Orlov N.V. 1988. Radioeng. and Electr. Acad. of Scie USSR. Nauka,

[17] R. Popovidi-Zaridze, G. Talakvadze, " Numerical Investigation of Resonant Properties of Metal-Dialectical Periodical Structures," Tbilisi State University, Institute of Applied Mathematics, Tbilisi, 1983.

[18] Barantsev R.G. Kozachjck V.V. 1968. Vestn. Leningrad. University (7) Mat. Mekh. Astron (2), 71-77.

[19] R. Zaridze, G. Lomidze and L. Dolidze, "Diffraction on a Dielectric Body Near the Surface of Division of Two Dielectric Mediums." Tbilisi State University Publisher, Tbilisi, 1989.

[20] Apeltsin V.F., Kyurktchan A.G. Relays hypothesis and analytical properties of wave fields. Radioengeneering and Electronics, 1985, v.30,N2,193-210.

[21] Kyurkchan A.G, 1986, Radioeng. and Electr. Acad. of Scie USSR. Nauka, v.31, N7, 1294-1303

[22] R. Popovidi-Zaridze, " The Method of Auxiliary Sources," Lecture Cycles, Academy of Science, Moscow, 1984.

[23] Popovidi-Zaridze R.S., Karkashadze D.D, Mtiulishvili K.A. Solution of the diffraction problems on the complicate shape body by method of composition. 7th Allunion Symposium of Diffraction and Wave Propagation. 1977, Moscow. v.3, 83-85 pp.

[24] Popovidi-Zaridze. R. S, Tsverikmazashvili Z. S. "Numerical solution of diffraction problem by modified method of non-orthogonal series," Journal of Applied Mathematics and Mathematical Physics, Moscow, 1977.

[25] R. Zaridze and D Karkashadze. " The Method of Auxiliary Sources and wave field singularities" Lecture Cycles, University of Kazan. 1988.

[26] Kupradze V. Method of integral equations in the theory of diffraction. 1935. Moscow-Leningrad.

[27] R. Popovidi-Zaridze., D. Karkashadze, G. Ahvlediani, and J. Khatiashvili, "Investigation of Possibilities of the Method of Auxiliary Sources in Solution of two-dimensional Electrodynamics Problems," Radiotechnics and Electronics, Vol. 22, No.2, Moscow, 1978.

[28] R. Zaridze and J. Khatiashvili, "Investigation of Resonant Properties of Some Open Systems," Tbilisi State University, Institute of Applied Mathematics, Tbilisi, 1984.

[29] R. Zaridze, D. Karkashadze, G. Talakvadze, J. Khatiashvili, Z. Tsverikmazashvili, "A Method of Auxiliary Sources in Applied Electrodynamics," URSI International Symposium of E/M Theory, Budapest , Hungary, 1986.

[30] Kopaleishvili V.P., Popovidi-Zaridze R.S. 1972 Radioeng. and Electr. Acad. of Scie USSR. Nauka v.27, N7. 1374-1381.

[31] Kopaleishvili V.P., Popovidi-Zaridze R.S. 1972 Radioeng. and Electr. Acad. of Scie USSR. Nauka v.27, N11, 2432-2435.

[32] Popovidi-Zaridze R.S. Karkashadze D.D., Khatiashvili J. 1981. Radioeng. and Electr. Acad. of Scie USSR. Nauka, v.36, N2, 254-262 pp.

[33] Zaridze R. Karkashadze D. Khatiashvili J. Method of Auxiliary Sources for investigation of along-regular waveguids 1985 Tbilisi State University 150 p.

[34] Jones D. S. Methods in Electromagnetic wave propagation. 1995. Oxford University Press joint with IEEE Press.

[35] Born, E. Wolf. Principled of Optic. 1965. Pergamon Press.

[36] Lourence Larsen, John Jacobi. Medical Application of Microwave Imaging", New-York, 1986.

[37] Zaridze R., Economou D., Jobava R., Uzunoglu N. A novel target imaging technique using the Method of Auxiliary Sources. Abstracts of International Conference on Electromagnetics in Advanced Applications, Torino, Italy, Sept. 15-18, 1997.

[38] R. Zaridze, G. Bit-babik , K. Tavzarashvili. "Analysis of the Scattered Field Singularities for Optimizing the Inverse Problems Solution". Proceedings of International Seminar/Workshop organized by Ukraine MTT/ED/AP *IEEE* chapter "Numerical Solution of Direct and Inverse Problems of the Electromagnetic and Acoustic Waves Theory (DIPED-97)". Lviv, Ukraine, Sept. 15-17, 1997 pp. 20-22. ISBN 966-02-0296-2.

[39] R.Jobava , R.Zaridze , D. Karkashadze, G.Bit-Babik, Ph.Shubitidze, The Methods of Auxiliary Sources for Two Dimensional Time Domain Scattering Problems. "Trans Black Sea Region Symposium on Applied Electromagnetism". Metsovo, Epirus Greece 17-19 April 1996 pp. DISC 4.

[40] Jobava R.G., Zaridze R.S., Karkashadze D.D., Shubitidze Ph.I., Development of the Method of Auxiliary Sources for Scattering Problems in Time Domain. "XXV-th General Assembly of international union of radio science, URSI.", August 28-September 5, 1996, Lille France, pp. 108.

[41] D.P. Economou, D.I. Kaklamani, R.Zaridze, V. Kouloulias, I.G. Tigelis and N.K.Uzunoglu. A Hybrid Method of Moments & Method of Auxiliary Sources (MOM/Method of Auxiliary Sources) Technique in Solving Complex Electromagnetic Structures. Proceedings of the International conference in Advanced Applications (ICEAA 97)September 15-18, 1997 - Torino, ITALY.

[42] Markov G, Vasiliev E. Mathematical Methods of Applied Electrodynamics. Soviet Radio, Moscow, 1970.

[43] Tikhonov A., Arsenin V. Methods for Solution the Non-correct Problems. Nauka, Moscow, 1974.

[44] Shiann-Jeng Yu, Ju-Hong Lee. Design of Two Dimensional Rectangular Array Beamformers with Partial Adaptivity. *IEEE Trans. AP-S*, vol. 45, NO 1, January 1997.

[45] Holt A.R., Uzunoglu N.K. and Evans B.G. "An integral Equation Solution to the Scattering of Electromagnetic Radiation by Dielectric Spheroid and Ellipsoid", *IEEE Trans. Antennas and Propagation*, AP-26, p.p. 706-712, 1978.

[46]. . Aleksidze M.A. Solution of boundary problems by expansion into a nonorthogonal series; 1978, Moskow, Nauka 351 p.